AN ABSTRACT OF THE THESIS OF

Lynn Gretton Dowding for the degree of Master of Science
(Name) (Degree)

in Oceanography presented on November 4, 1975
(Major) (Date)

Title: SEDIMENTATION WITHIN THE COCOS GAP, PANAMA BASIN

Abstract approved: Redacted for Privacy
Tjeerd H. van Andel

The Cocos Gap is a deeper portion, or saddle, of the Cocos Ridge and forms part of the western boundary of the Panama Basin. It is probably typical of saddles within most submarine ridges. In order to determine the mechanisms controlling sediment dispersal, the nature and sources of the sediments at 23 core locations were defined by hydrodynamic size separation (> 63, 2-63, < 2 micron) and microscopic or X-ray diffraction analysis of the individual fractions. In addition, calcium carbonate, organic carbon, opal and quartz determinations were made for the total sediment.

The silt-sized fraction was resolved into eight textural modes. The coarse modes reflect the progressive breakage and winnowing of the corase fraction (foraminifera) under the influence of bottom currents and gravity. Above 2000 m mechanical breakdown, winnowing and relocation by bottom currents mask the effects of depth related

dissolution of the carbonate fraction. Intermediate modes in general represent a transitional facies with both biogenic and terrigenous influences, while the finest modes characterize a distal regime of clay deposition. The clay fraction is amorphous material with very low percentages of well crystallized clays. Three main sources and transport paths were recognized, including one associated with the circulation of the Panama Basin.

Sedimentation within the Gap is controlled by local processes, predominantly the interaction between tidally induced intensification of bottom water flow and directional (thermohaline) flow. The steepness of the sea floor slope is a major factor controlling the efficiency of winnowing of the sediment away from certain higher elevations (biogenic source areas) to the sheltered parts and flanks of the ridge. Superimposed upon this sediment dispersal is the influx of terrigenous material carried by directional bottom currents that operate as postulated upper and lower contour currents along the flanks of the ridge.

The crest of the Cocos Gap acts as a catchment area for the biogenic components, while the adjacent more sloping region, the sub-plateau, acts as a source area. The extreme breakage of the foraminifera is most likely a function of the tidally induced intensification of the bottom water flow, characteristic of many shallow ridges, and is probably most significant in the sub-plateau. Hydrographic data indicates that there is no significant transport of bottom water across the Cocos Gap into the Panama Basin, but downslope transport of carbonate and siliceous fragments and minerals from the Gap into the basin is associated with cyclical tidal bottom water flow.

Sedimentation Within the Cocos Gap, Panama Basin

by

Lynn G. Dowding

A THESIS

submitted to

Oregon State University

in partial fulfillment of
the requirements for the
degree of

Master of Science

Completed November 4, 1975

Commencement June 1976

APPROVED:

Redacted for Privacy

Professor of Oceanography
in charge of major

Redacted for Privacy

Dean of School of Oceanography

Redacted for Privacy

Dean of Graduate School

Date thesis presented November 4, 1975

Typed by Margie Wolski for Lynn G. Dowding

ACKNOWLEDGEMENTS

I would like to thank Dr. Jerry van Andel for acting as my advisor, and offering support and encouragement at critical times throughout the preparation of this thesis. Dr. Jorn Thiede deserves special thanks for his suggestions and guidance during the final stages, and for serving on my committee with very short notice when illness forced Dr. Julius Dasch to miss my oral examination. My thanks are also extended to my other committee members, Drs. Dasch, Jack Corliss, and Art Boucot for their suggestions and interest in this project.

I appreciate the assistance received from Pat Price, who helped me with the opal/quartz analyses, and Elizabeth Asbury and Carla Rathbun, who provided the carbonate values. Milo Clauson introduced me to the intricacies of the Cahn Electrobalance and X-ray machine, and I am grateful for the instructions he gave me for the techniques this thesis incorporated. Smear slide faunal data was provided by Dr. Ted Moore and Chiye Wenkam (Yamashiro) quantified the compositional fractions of certain grain size modes.

I have benefitied immensely from discussions with the faculty and students, particularly Chiye Wenkam, Terry Chriss, Steve Swift, Drs. David Rea and Des Barton. I thank Margie Wolski for typing this thesis and Kathryn Torvik, Alison Webber, and David

Reinert for assistance with the figures. Finally I wish to thank my family for their constant support, letters and prayers during the time I have been in Corvallis and during the other times of separation.

This research was funded by a grant of the Office of Naval Research (N00014-67-A-0369-0007) and utilized samples from cores collected under grant N00014-67-A-0108-004 and National Science Foundation Grant GA-35454.

TABLE OF CONTENTS

LIST OF FIGURES

LIST OF TABLES

SEDIMENTATION WITHIN THE COCOS GAP, PANAMA BASIN

INTRODUCTION

The Panama Basin is a morphologically distinct portion of the Cocos Plate that includes many geological features of a typical ocean basin, but on a more easily studied scale. Its small size, large variations in water depth and proximity to the continental margins of Central and South America produce steep lateral gradients in the character of both pelagic and hemi-pelagic sediments. This permits unusually complete insight into a variety of aspects of deep sea sedimentation.

The Panama Basin lies in one of the most biologically productive regions of the world, under the eastern part of the Pacific Equatorial Current system. Consequently, calcareous and siliceous components are supplied in abundance. In addition, the basin receives clay and silt-sized terrigenous material and volcanic input from the continental margins (Heath and others, 1974; Bowles and others, 1973; Ninkovich and Shackleton, 1975).

Previous studies (van Andel *et al.*, 1971; Moore *et al.*, 1973; Heath *et al.*, 1974; Kowsmann, 1973; van Andel, 1973; Yamashiro, 1975) have shown that sedimentation within the basin is dominated by four processes: 1) input of biogenic and terrigenous material,

2) dissolution of calcium carbonate, 3) winnowing of sediments on the ridge and transport of the fine material into deeper water, and 4) the transport of fine sediment by currents from the eastern to western parts of the basin.

The Cocos Gap (Fig. 1) is a saddle on the Cocos Ridge and a key location for a study to understand the processes of sediment redistribution within a typical ridge environment. The bases for this study are bathymetric and sediment isopach maps, hydrographic data and analyses of the texture and composition of the sediment at 23 core locations (Fig. 2). The data and samples for this study were obtained during cruise YALOC-71 on the R/V Yaquina of Oregon State University, and from a site survey of Deep Sea Drilling Project Site 158 by R/V Vema (cruise Vema-28, Truchan and Aitken, 1973). In addition, bathymetric, seismic reflection and core data from the previous regional surveys were available.

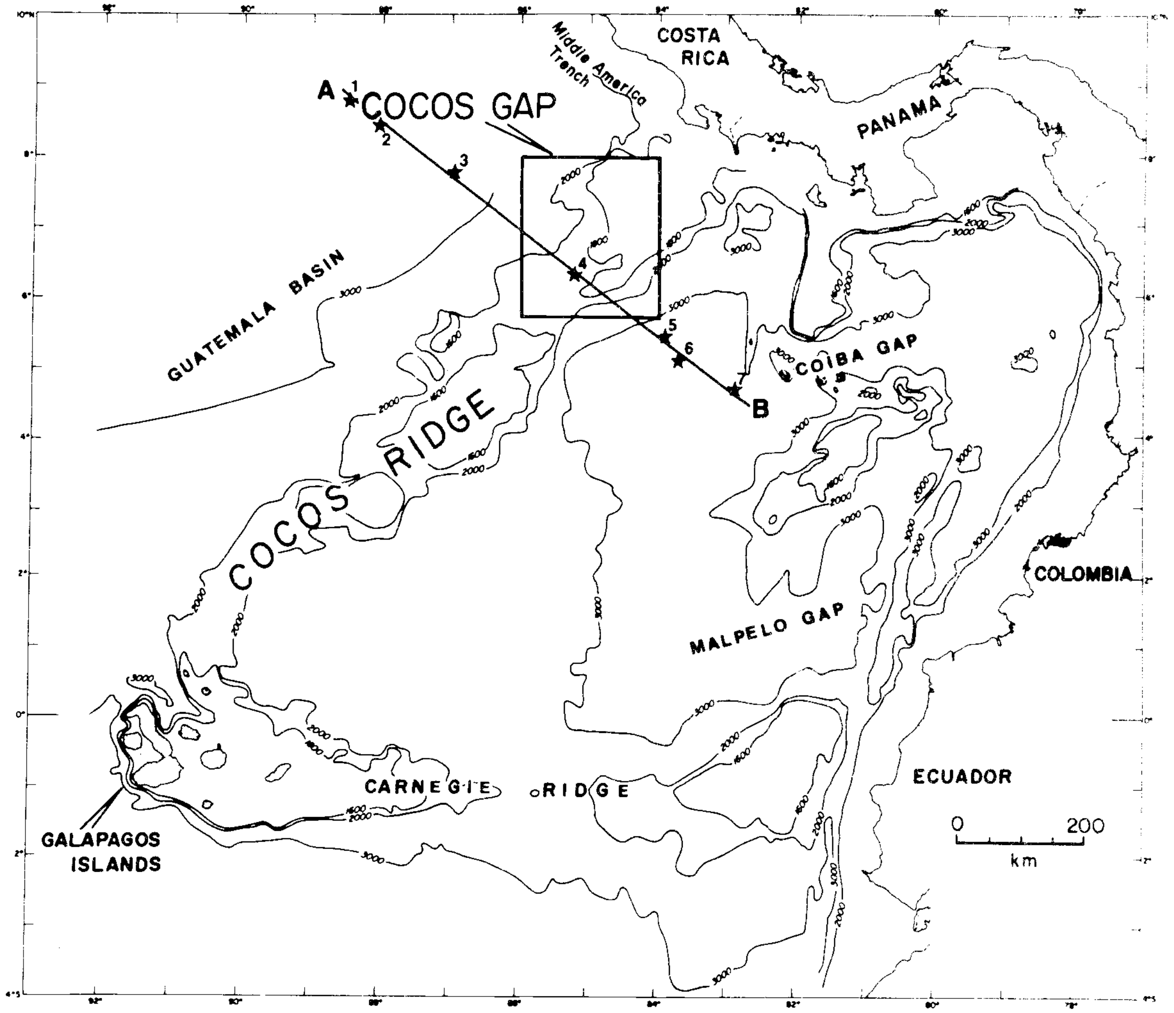

Figure 1. Bathymetric map of the Panama Basin showing the Cocos Gap. A-B: location of potential density profile of figure 5. Contour interval: 1600, 2000, 3000 meters (uncorrected for variations of sound velocity with water depth).

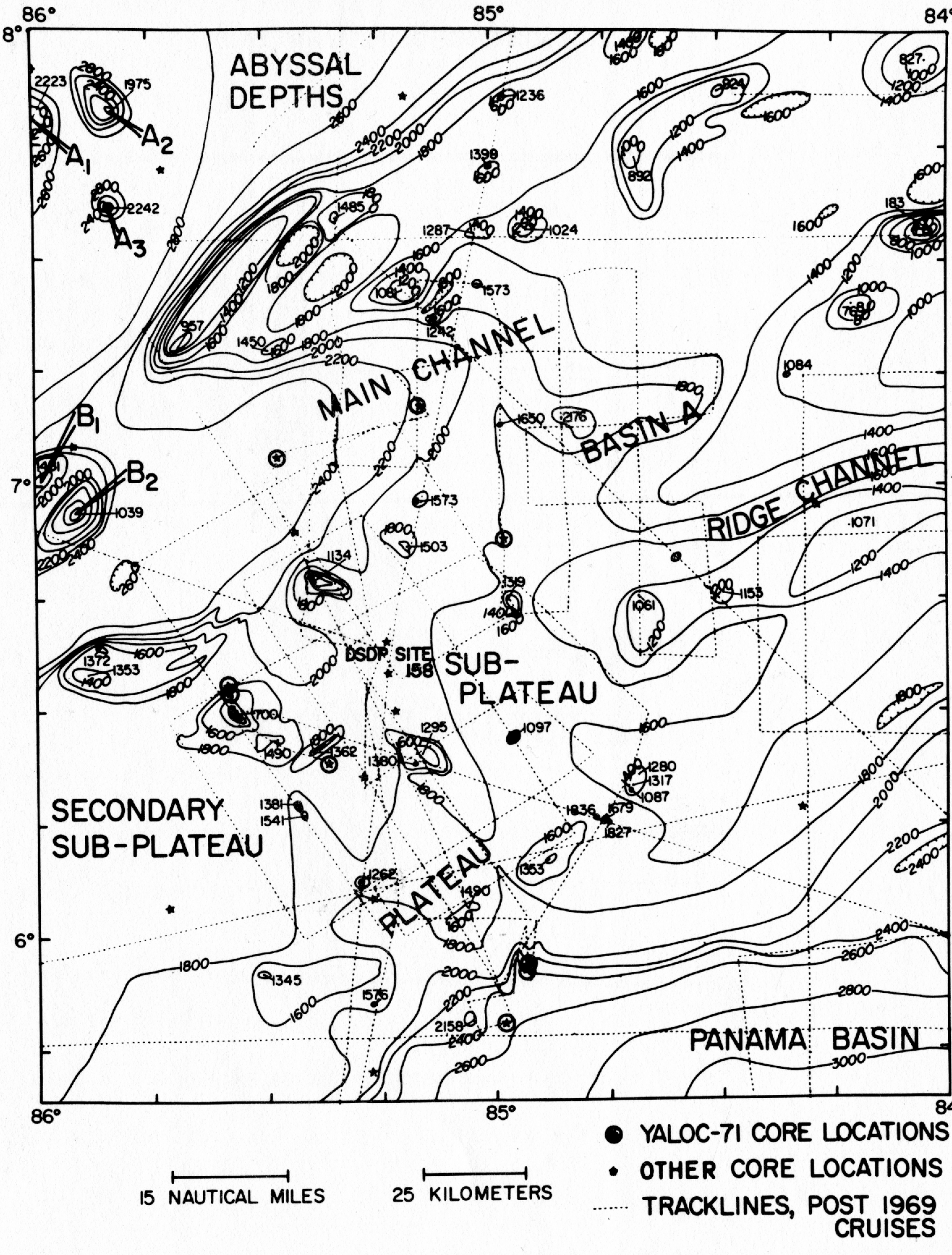

Figure 2. Bathymetric map of the Cocos Gap, showing the main topographic regions. Contour interval: 200 meters (corrected).

TOPOGRAPHY OF THE COCOS GAP

The Cocos Ridge is an aseismic submarine feature with a depth range from sea level (Cocos Island) to 2000 m. It is the western boundary of the Panama Basin and extends southwestwards from the continental margins of Costa Rica, where it terminates the Middle America Trench, to the Galapagos Islands. The ridge is divided into several topographically distinct blocks by three deeper areas or saddles, the northernmost one being the Cocos Gap (Fig. 1). Several topographic regions reflecting the complex structural history can be recognized (Fig. 2) (van Andel et al., 1971; Bentley, 1974).

In the north, the Guatemala Basin is flat, with the exception of three isolated hills (Fig. 2). The northern part of the ridge has a series of northeast-southwest trending seamounts and basins, the most prominent being the basalt ridge that abruptly rises 2000 m from the abyssal depths as a shear cliff (Fig. 2).

The northern seamount chains are separated from the main part of the Cocos Ridge by a relatively broad, smooth-floored channel (Figs. 2, 3) sloping quite steeply to the southwest. South of the main channel lies the sub-plateau region which averages 1800 m and slopes gently to the northeast. Its northern part is a basin (A: Fig. 2) which is separated by a major fault from the main channel (Fig. 3). To the east of the sub-plateau, the Cocos Ridge rises quite steeply and the

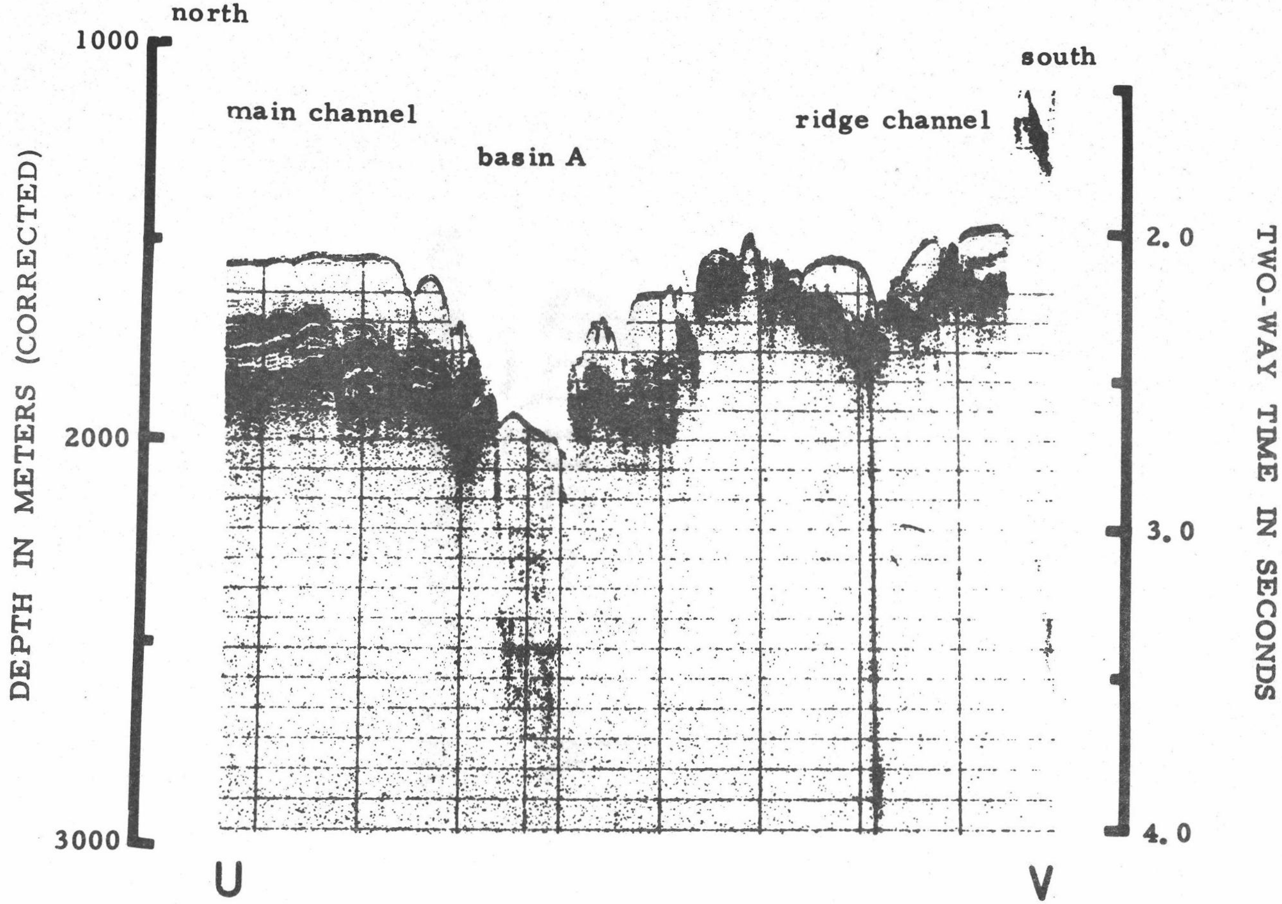

Figure 3. Airgun reflection profile across basin A. Location of profile shown on Figure 6.

terrain is relatively rough. At about 7°N there is a narrow channel (Figs. 2, 3) trending east-northeast - west-southwest at the elevation of the sub-plateau. South of this ridge channel at about 84°45'W is a north-south line of peaks, basins and sediment mounds (line A-B, Fig. 4). At point A this north trending line meets two other seamount chains: A-C and A-D. Line A-C separates the sub-plateau from the plateau line A-D is the southernmost and highest part of the plateau.

The crest of the Cocos Ridge (plateau: Figs. 2, 4), in places only a few kilometers wide, lies at 1800 m and is level with local peaks and depressions. Two main channels cut into the plateau from the north and south. Other channels, described by Wilde (1966), occur in the extreme southwest portion of the plateau and in the relatively featureless secondary sub-plateau (Fig. 4), which occurs west of the plateau and slopes gently towards the abyssal plain. South of the plateau, the flanks of the Cocos Ridge slope more gently than the steep northern wall.

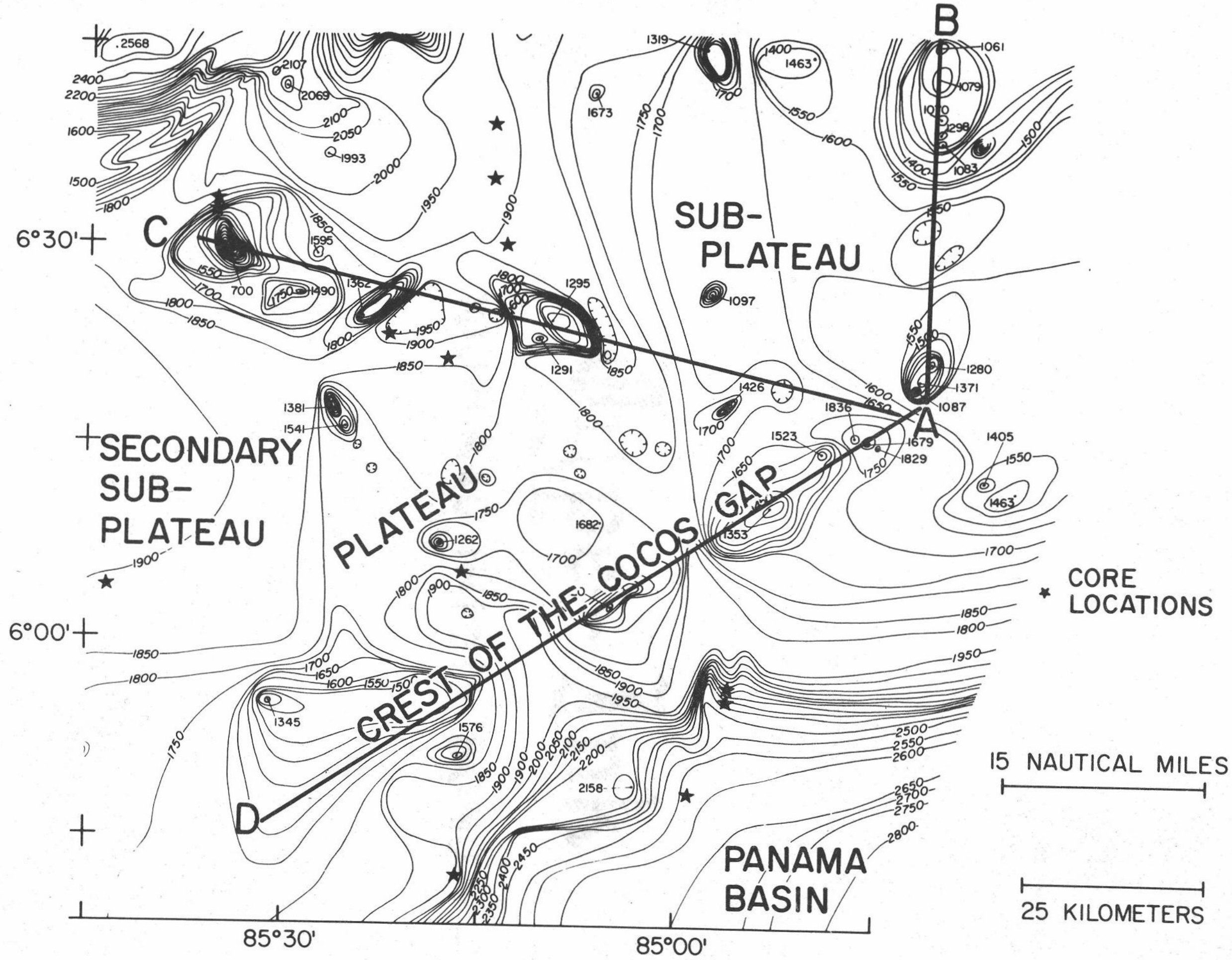

Figure 4. Bathymetry of the crest of the Cocos Gap. A-B, A-C, A-D: seamount chains mentioned in the text. Contour interval: 50 meters (corrected).

PHYSICAL OCEANOGRAPHY OF THE COCOS GAP

The surface circulation of this part of the Panama Basin involves the eastern extremities of the Equatorial Counter Current and the North Equatorial Current. Through the survey area the two currents interact via cyclonic flow of the countercurrent around the Costa Rica Dome. The location and intensity of the Dome fluctuate seasonally with changes in the major wind systems, predominantly the Inter-Tropical Convergence Zone (ITCZ).

From July to December when the Equatorial Countercurrent is well developed, the surface flow through the survey area is predominantly to the east or northeast. From January to March the ITCZ is farther south, the Equatorial Countercurrent is absent and the dominant flow in the area is southwestward around a large gyre centered within the survey area. During April to June an eastward flow develops (Wyrtki, 1965).

The sub-surface circulation within the Panama Basin probably consists of a pattern of eddies and closed cells that is the result of the mixing of the surface waters with the eastward flowing Equatorial Undercurrent just to the south of the survey area (Pak and Zaneveld, 1973; Stevenson and Taft, 1971).

Influx of deep water into the Panama Basin occurs at about 2500 m between the eastern end of the Carnegie Ridge and the continental margin of Peru. From there, it spreads northwards into the eastern part of the basin and thence westwards through the deep Malpelo and Coiba gaps (Fig. 1) into the western part (Laird, 1969, 1971; Kowsmann, 1973). The main outflow of water is probably over the lowest parts of the Carnegie Ridge (Kowsmann, 1973).

Hydrographic stations (Wyatt et al., 1969; Kowsmann, 1973) on the Cocos Ridge provide transverse and longitudinal hydrographic sections of density, salinity, temperature and oxygen variations. Temperature-salinity plots indicate that there is no difference between water mass characteristics to the north and south of the ridge in this locality which suggests there is no inflow or outflow of bottom water across the Cocos Gap.

Higher oxygen concentrations and lower temperatures in the near bottom water occur outside the Panama Basin than inside, but only the density transverse section (Fig. 5) showed significant variations in gradients. Kowsmann (1973) suggested that under a tidal influence bottom water flow was possible into the basin because the potential density gradients are greater outside than inside the basin. However, the density differences (Fig. 5) are small and, although the bottom water flow is likely to be in response to cyclical reversals of tidal currents, there is little evidence for a directional system of bottom water flow into the basin driven by density contrast.

South of the Cocos Gap, the downwarping of the isopycnals

(Fig. 5), and corresponding small changes in temperature, oxygen and salinity profiles indicate there is bottom water flow parallel to the flanks of the Cocos Ridge. Therefore, as the flow is parallel to the contours and is associated with the thermohaline circulation within the basin, it can be called a contour current (Heezen and others, 1966). Its existence was postulated from coarse fraction data (Kowsmann, 1973) and clay mineralogical data (Heath et al., 1973). Through the abyssal depths the bottom water flow parallels the regional trend of the ridge but its distance from the ridge flanks indicates that it is not a contour current. Within the Cocos Gap, channels in the sediment (usually about 100 m deep, Fig. 3) indicate that bottom currents are actively flowing through the area and are controlled by topography.

The flow pattern through the area is probably complicated by cyclical tidal reversals as other studies have shown that normal tidal flow in the deep sea is accentuated in areas that are relatively shallow. For example, while tidal velocities at abyssal depths are usually of the order of 1-5 cms per second (Isaacs et al., 1966; Nowroozi et al., 1968), velocities of up to 25 cms per second were recorded at depths of 2.7 km on the Galapagos spreading center (Detrick et al., 1974). These high velocities were not associated with a definable thermohaline circulation; rather the bottom currents may be accelerated because the angle of the slope of the sea floor

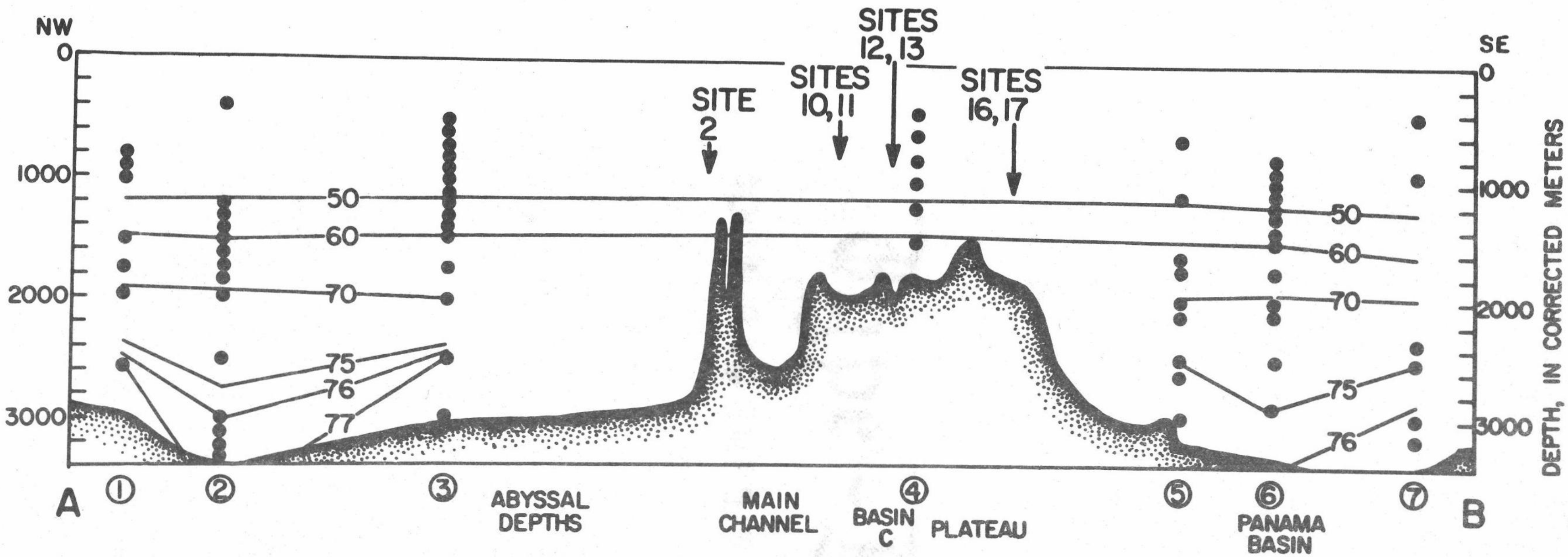

Figure 5. Potential density across the Cocos Gap. Contours are: (potential density - 27) x 100 ; ie. 60=27.60. Control points are shown by black dots. Location of profile shown on Figure 1.

equals the angle of inclination of the energy flux of the internal wave (Sandstrom, 1966, 1969; Wunsch, 1969). Within the relatively flat plateau and sub-plateau regions this may be a significant factor; the extensive destruction of biogenic particles discussed later and the occurrence of channels in the sediment indicate appreciable current velocities.

SEDIMENT THICKNESS IN THE COCOS GAP

Approximately 60% of the central survey area is covered with sediment, mainly as undulating infillings of basement depressions (Figs. 6, 7a). Groups of small volcanic hills, isolated seamounts and occasionally uplifted basement blocks are barren pavements (Fig. 7a).

Thin sediment (<0.1 seconds) occurs as patches, but thicker deposits (> 0.2 seconds) show six distinct accumulations corresponding to the topographic regions (Fig. 6). The main channel, basin A and the sub-plateau, are separated by basement ridges associated with major faults. Thicker sediment fills (> 0.3 seconds) identify several isolated basins (Fig. 6: Basins A, B, C, at least one basin within the eastern ridge crest area) and the secondary sub-plateau and the ridge flanks also have thick sediment cover, but the most prominent accumulation feature is the main channel (Fig. 13). This is made up of six en echelon basins that do not have any topographic expression (Fig. 6).

The sediment distribution (Fig. 6) indicates areas of selective sediment accumulation alternating with areas of non-deposition or scouring. Most of the hills within the survey area have small moats associated with them (Fig. 7b), similar to those described by Johnson and Johnson (1970). Occasionally sediment is piled adjacent

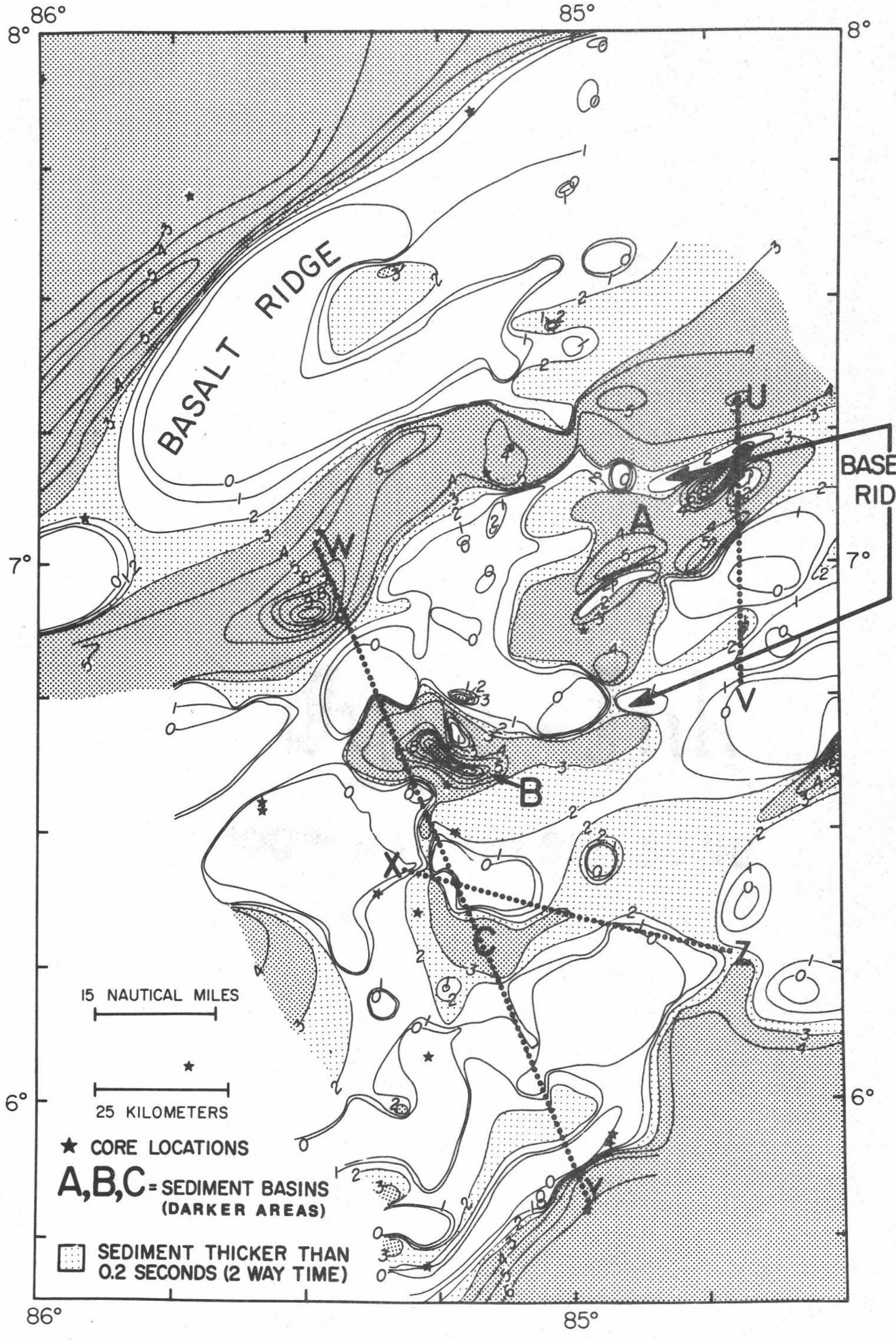

Figure 6. Distribution and thickness of sediment overlying accoustic basement. U-V, W-X-Y, X-Z : location of reflection profiles of figures 3 and 7. Contour interval: 0. 1 seconds., two-way time.

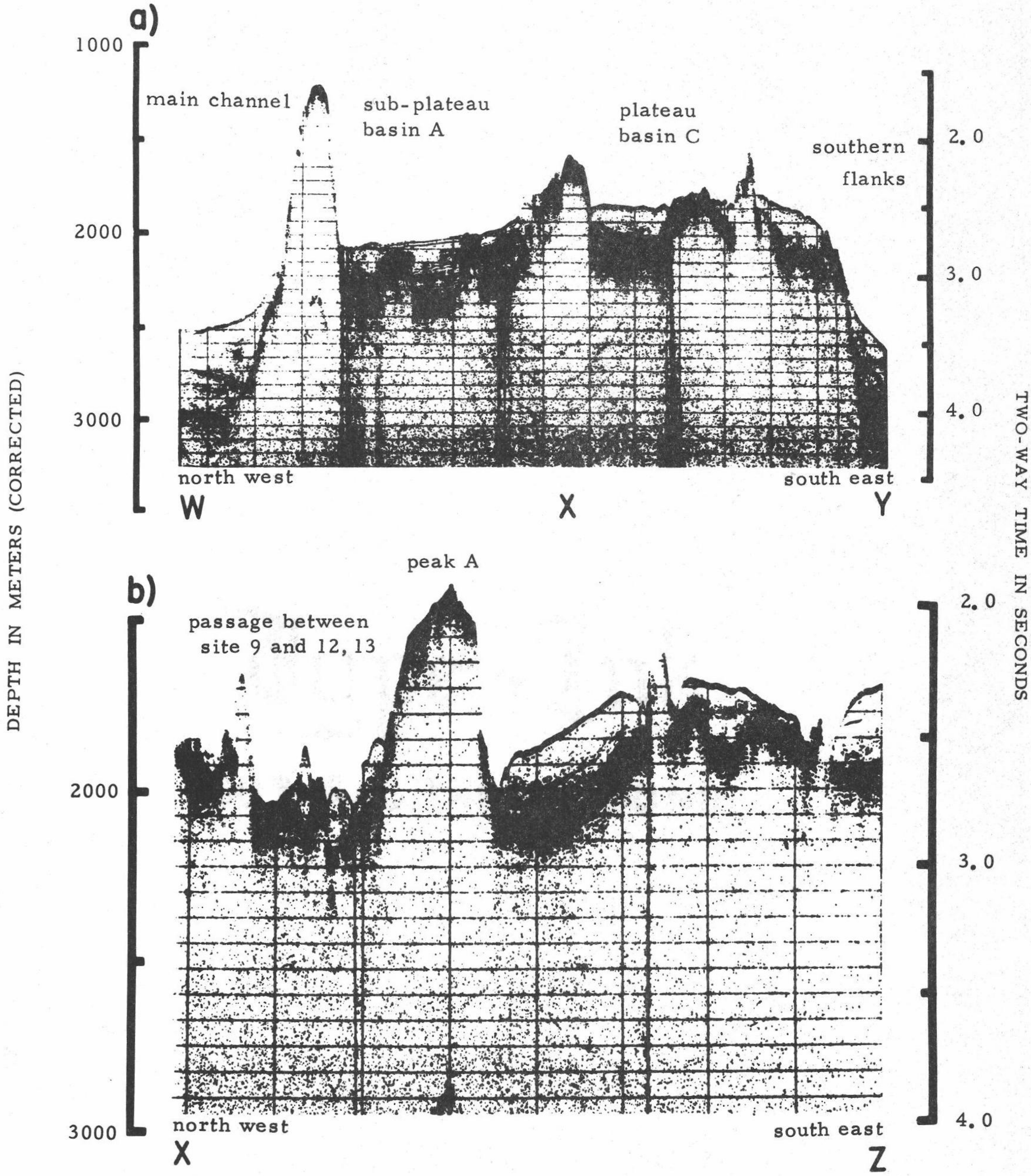

Figure 7. Airgun reflection profiles. a) W-X-Y: across the Cocos Gap b) X-Z: across the Cocos plateau. Location of profiles shown on figure 6.

to the hills (Fig. 7b, peak A), however, the basins have remarkably flat surfaces (Fig. 7a) and there is no evidence that they are accumulations of sediment to the leeside of the hills. Initially, depressions (mostly grabens) in the basement acted as traps for the sediment, but now infilling is largely complete and the smoothed topography controls the sediment transport paths. Numerous small channels are cut into the undulating sediment floor suggesting that the bottom water flow through the area is channelized into networks of depressions, with local restrictions between seamounts. Such restrictions are often characterized by the underlying sediment forming mounds with channels cut into them (Fig. 7b, passage way between sites 9, 12, 13).

LITHOLOGY OF THE COCOS GAP SEDIMENTS

The sediments of the Cocos Gap are mainly olive gray calcareous oozes, commonly mottled, but uniform from region to region without major lateral color or textural changes, except that in the main channel clayey rather than silty sediments predominate. At depth in the cores, clay- and silt-sized layers alternate, sometimes as fine laminations and occasionally with accompanying color changes, for example site 18. Lighter colored pockets of foraminiferal sand are common, especially at sites 4 and 20. Although slumping is likely, associated with the major faulting recognized from the air gun records (see Fig. 7a), no oceanic turbidites, as described by Wilde (1966) were found.

The dominant biogenic component of the surface sediment is calcium carbonate; about 30% of the carbonate-free residue is opal. Clay is the main terrigenous material present, with small amounts of organic carbon and quartz. Other sedimentary components are volcanic shards and some non-clay minerals. Compositional data are given in Table 1.

Most of the cores within the Cocos Gap have burrows preserved in them that are the same color as the overlying sediments and texturally similar although occasionally consisting of finer grained material. Frequently the burrows are lined with foraminifera and

TABLE I. Sample Identification and Compositional Data.

Core No.	Core Identification	Latitude °N	Longitude °W	Water Depth (corrected meters)	Carbonate % of total sample	Opal % of total sample	Opal % of $CaCO_3$ free sample	Detritus % of total sample	Quartz % of opal $CaCO_3$ free sample	Organic** carbon % of total sample
1	V15-17	7.55	86.00	3078	0.3	25.6	25.7	74.3	7.1	1.8
2	V15-28	7.05	85.55	2400*			25.7		9.2	1.9
3	Y71-3-2	7.10	85.09	2164	6.7	28.5	30.6	60.6	9.8	3.2
4	Y71-3-3	7.03	85.30	2551	2.2	35.3	36.1	62.9	9.2	3.2
5	V28-34	6.54	85.26	2434	9.7	24.9	27.6	66.4	7.7	2.9
6	Y71-3-1	6.53	84.58	1824	9.1	31.0	34.1	53.0	10.6	3.6
7	V20-15	6.57	84.17	1736	18.7	18.5	22.8	64.0	8.8	
8	V28-138	6.35	85.14	1972	21.5	21.7	27.7	55.9	10.1	2.9
9	V24-36	6.30	85.13	1878	51.0	13.7	28.0	35.7	9.0	
10	Y71-3-7FF1	6.34	85.35	1765	46.1	17.6	32.6	36.3	9.0	2.2
11	Y71-3-7FF2	6.33	85.35	1631	36.4	17.7	27.9	45.5	9.7	2.9
12	Y71-3-6	6.23	85.22	1945	35.6	21.1	32.7	43.2	10.1	2.9
13	V15-29	6.21	85.17	1889	65.9	4.6	13.6	29.5	7.1	
14	V18-349	6.04	85.43	1818			32.6		9.8	8.2
15	V28-135	6.05	85.16	1778	63.9	11.8	32.6	24.1	11.0	1.4
16	Y71-3-5FF3	5.56	84.56	2244	20.0	27.9	34.9	52.1	9.7	3.6
17	Y71-3-5FF5	5.55	84.56	2363	14.8	33.5	39.3	51.8	10.2	4.1
18	Y71-3-4	5.48	84.58	2628	12.1	32.7	37.2	55.2	9.4	3.3
19	RC10-150	6.17	84.19	1734	14.8	33.5	39.3	34.2	8.5	
20	V18-350	5.42	85.16	1838	74.8	7.1	28.1	18.2	9.2	
21	DSDP-158	6.37	84.14	1953	51.0					
22	P-HF-19	7.51	85.11	2512	19.1	23.1	28.5	58.2	9.5	
23	P-HF-27	7.42	85.43	2990	11.7	28.1	31.8	60.3	7.6	

* core description depth: 2860 m, depth from bathymetry map: 2400 m.

** measured by LECO model 714 carbon analyzer, using a controlled oxidation technique to distinguish between total carbon and organic carbon. Error estimate: ± 10% of organic carbon present.

radiolarian spines. Two morphologies were found in the YALOC-71 cores: the first, filled with uniform light colored sediment and found in the plateau and sub-plateau, was probably formed as the paler overlying sediment was sucked into the burrow following the forward motion of such organisms as polychaete worms. The second type, predominantly found in the main channel, is an ordered packing of alternate light and dark colored sediment that is probably a mixture of fecal pellets and sediment that was passed over the body of the burrower. Echinoids probably produced some of these burrows but as their respiratory tube feet must always stay in contact with the water they could not have formed those that are found up to 50 cm below the ancient sediment/water interface. These were probably formed by crustaceans. Along the southern flanks of the ridge both groups occur.

The separate distributions of the two morphologies suggests that they are genetically distinct. A third group, characterized by serrated edges, occurs at site 18 and it may represent examples of very well preserved type 1 burrows or indistinct type 2 burrows. Similar morphologies were recognized by Donahue (1971): type 1 corresponds to his "simple" group, while type 2 is similar to the sketch but not the photograph of his "imbricate" type. It also resembles Seilacher's (1967) "zoophycos burrowing."

Biogenic Components

Calcium Carbonate Distribution

Calcium carbonate was measured using a LECO model 714 carbon analyzer, with an approximate error of ± 2% of the calcium carbonate present, for carbonate values over 8%.

Calcium carbonate becomes increasingly soluble with depth, as temperature decreases and pressure increases; the two significant levels being the Lysocline and the Calcite Compensation Depth (CCD). The Lysocline is the level where the rate of dissolution increases abruptly (Berger, 1968, 1970) and below which major fluctuations in solution intensity occur (Luz and Shackleton, 1975). Just south of the Cocos Gap at 4°6.3'N, 85°0.1'W, the Lysocline is found between 300 and 1500 m (C. Yamashiro, personal communication). The CCD is found at a greater depth and is thought to be a geological facies change level rather than a chemical change as it represents the level of total carbonate dissolution (Heath and Culberson, 1970; Morse and Berner, 1972). Within the Panama Basin the CCD is about 3400 m but it rises 150 to 400 m nearshore (Moore _et al._, 1973). Therefore, within the Gap all the sites lie between the Lysocline and the CCD, which is significant in terms of the ease at which the foraminifera are fragmented and the proportions of carbonate dissolved.

Although there is a general decrease in carbonate content with depth, the distribution pattern (Fig. 8a) does not fit a simple depth related dissolution relationship. The variations in carbonate content for any given depth suggests that rapid downslope transport occurs, with limited accompanying dissolution. In addition, a few sites (group III, sites 6, 7, 8, Fig. 8b) in shallow locations have little carbonate and imply that significant dilution with non-calcareous material must occur. Sites with high carbonate values (group I, Fig. 8a) are found in the plateau (> 60%), sub-plateau and site 19 (> 40%). The lowest carbonate values (group II, Fig. 8a) correspond to the main channel and site 1, in the abyssal depths.

Opal Distribution

The opal content of the sediment was determined by X-ray diffraction using the cristobalite conversion technique (Goldberg, 1958; Calvert, 1966), following the procedure developed by Ellis (1972). The values are expressed as weight percentages of the total sediment, with carbonate-free values also given (Table 1) as additional data to indicate the masking of the opal by carbonate. The error is ± 5% of the opal present.

The opal distribution pattern (Fig. 9a) is scattered, with the highest values along the southern flanks of the ridge, basin A and deepest part of the main channel. The lowest values correspond to the plateau, but after eliminating the masking effect of carbonate a)

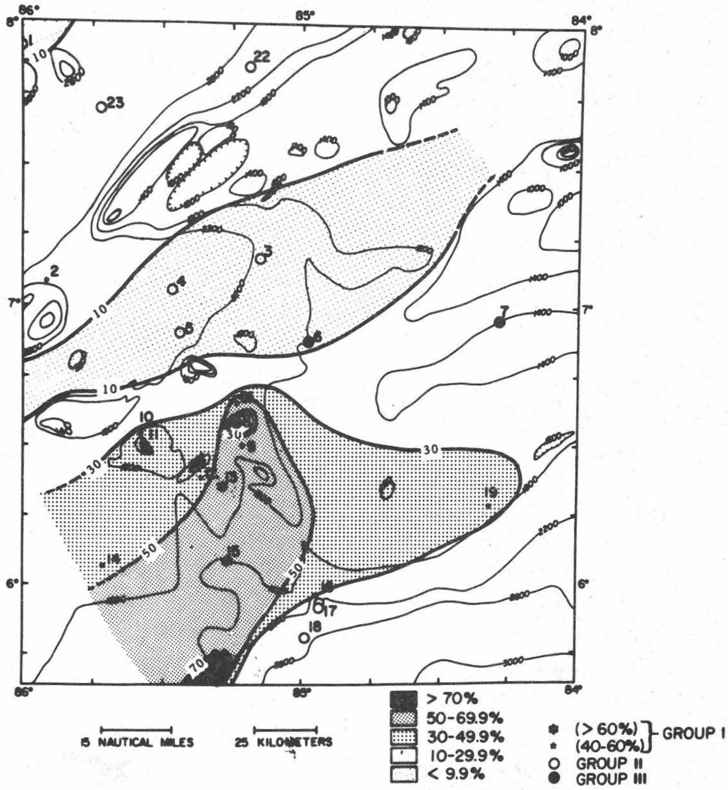

b)

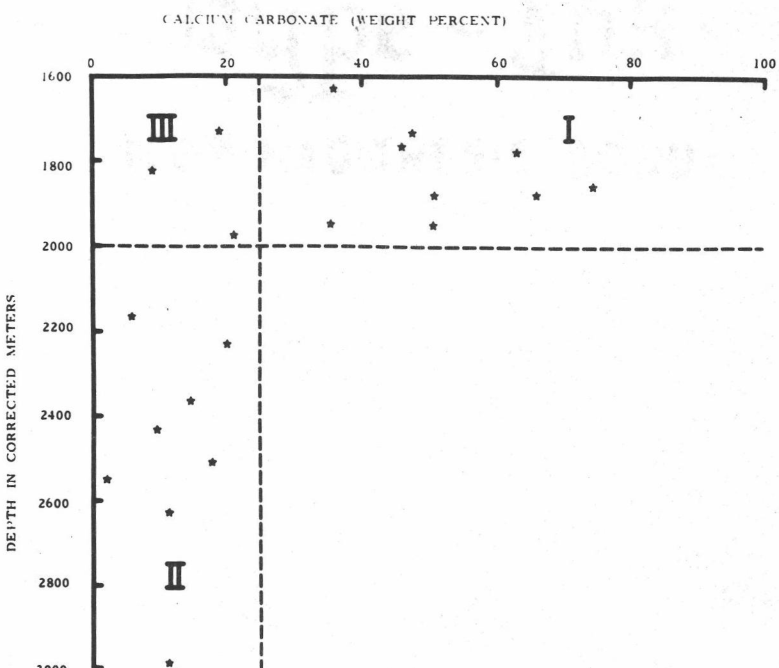

Figure 8. **a) Distribution of the calcium carbonate content of the surface sediments. b) Calcium carbonate content of the surface sediments vs. water depth. (in weight percent of total sediment)**

Figure 9. Distribution of opal in the surface sediments: a) weight percent of total sediment, percentages near stations are the percent radiolaria in the coarse fraction b) weight percent of carbonate - free sediment.

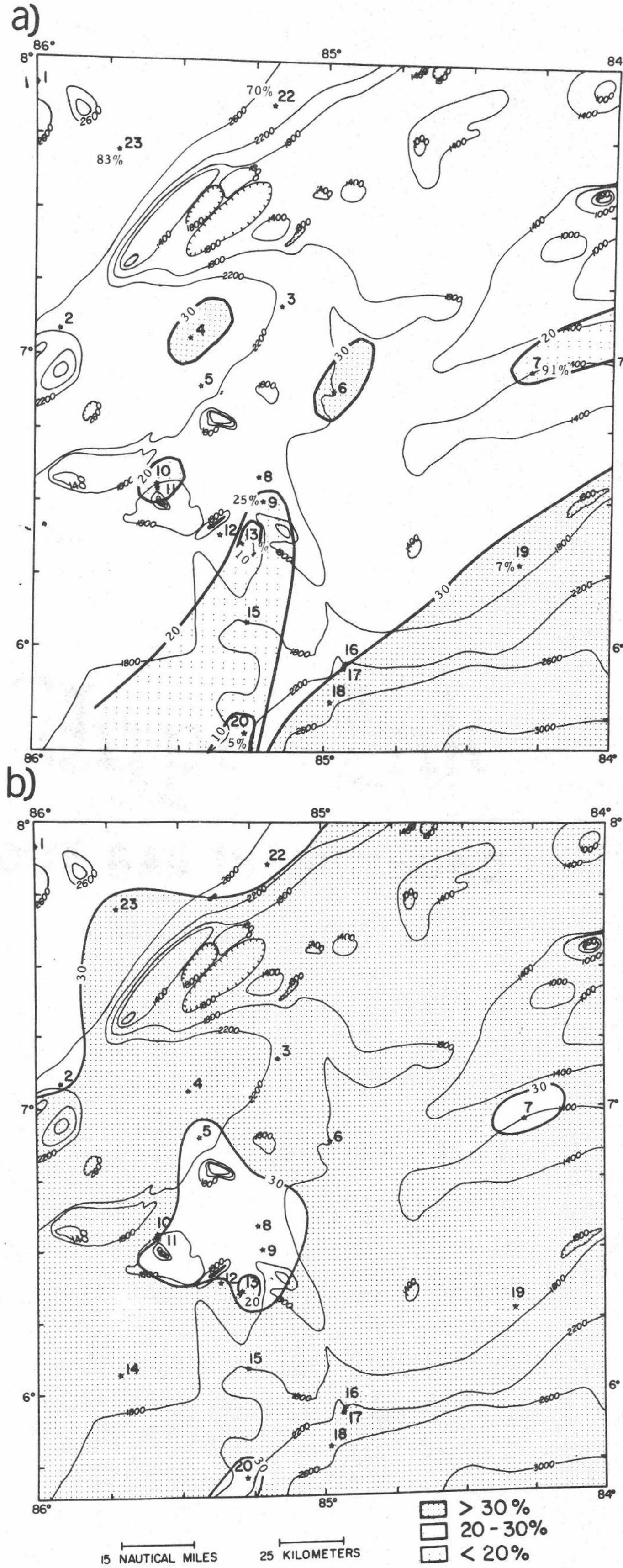
a)
b)
86°
85°
84°
8°
7°
6°
70%
83%
91%
25%
7%
5%
> 30%
20 - 30%
< 20%
15 NAUTICAL MILES
25 KILOMETERS

values, the lowest values are found predominantly in the sub-plateau (Fig. 9b). Considering adjacent cores, there is a tendency of the opal content to increase downslope, and accumulate at the foot of the ridge flanks in opal-rich chaff zones (Moore et al., 1973).

Most of the opal is fine-grained as only small percentages of diatoms are found in the coarse fraction and the distribution of radiolaria (Fig. 9) is not correlated with opal abundances. This also suggests that the agents of deposition of the fine and coarse fractions are different.

Terrigenous Components

Detritus Distribution

Detritus is defined as the terrigenous residue after removal of calcium carbonate and opal. It predominantly consists of clay minerals and quartz and is found mainly to the north of the sub-plateau and along the southern flanks of the ridge (Fig. 10).

Clay mineral determinations were made on the YALOC-71 cores but as the material was poorly crystallized or amorphous, the identifiable clay minerals occurred in small amounts and no mapable patterns were found. As part of this procedure, opal-rich detritus grain size determinations were made. However, as the relatively uniform carbonate-free opal distribution (Table 1) does not

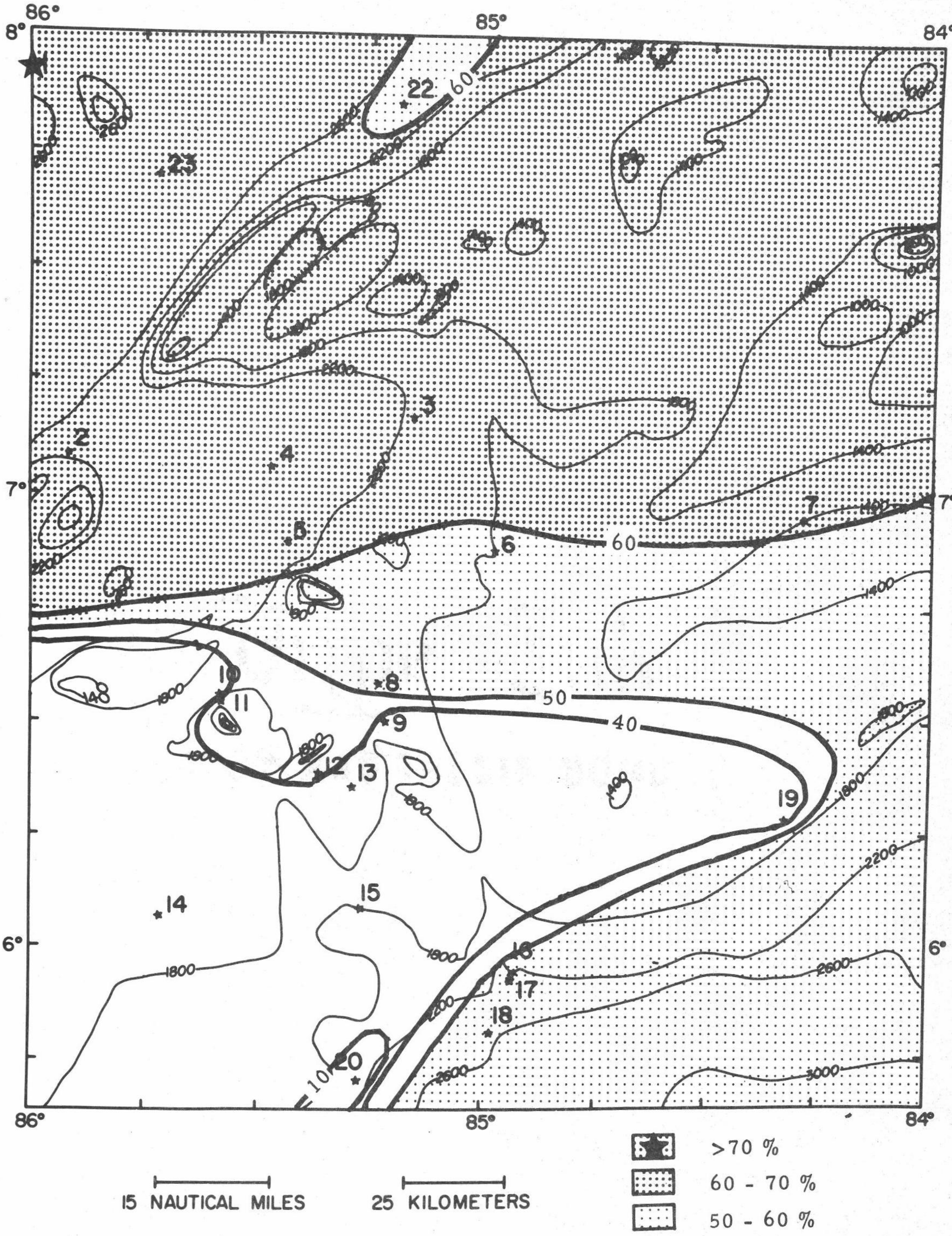

Figure 10. Distribution of detritus in the surface sediments (weight percent of total sediment).

correspond to the detritus distributions, the opal values do not significantly mask the detritus grain size determinations.

In general, the sand-sized fraction (> 63 micron) forms less than 8% of the sediment. It consists of quartz grains and volcanic shards, with the highest values at sites 10, 11, and 16, and the lowest values in the main channel, basin A and site 17. The silt-sized fraction (2-63 micron) is uniformly distributed (36%) except for higher values in basin A (39%) and lower values along the southern flanks of the ridges (31-33%). The opal-rich clay-sized detritus (< 2 micron) percentages were higher for the main channel and southern flanks (63%) than for the plateau and sub-plateau (58%). This suggests that both silt and clay-sized terrigenous material enters the main channel while the postulated contour current transports mainly clay-sized particles.

Quartz Distribution

Quartz determinations were made simultaneously with the opal determinations (Ellis, 1972), and are expressed as weight percentages of the carbonate- and opal-free sediment to avoid masking the quartz values by the biogenic components. The error for the values is ± 2% of the quartz content of the sediment.

Quartz is a good indicator for both aeolian and terrigenous input (see for example, Rex and Goldberg, 1958; Heath, 1975). In the

Panama Basin, however, the waterborne quartz, derived from Colombia, Ecuador, and Nicaragua (Heath et al., 1974), is trapped in the eastern Panama Basin (Plank et al., 1973; Heath et al., 1974) and the Middle America Trench. In addition, the aeolian input for this region is small (Prospero and Bonatti, 1969) so the quartz values are expectedly low and the input is likely to be uniform for the area as a whole.

The distribution pattern for quartz (Fig. 11) is approximately the opposite of the opal pattern (Fig. 9) as the highest values correspond to the plateau and sub-plateau. In addition, high values are found in basin A and at site 17, on the southern flanks of the ridge. The lowest values occur in the abyssal depths, southern part of the main channel and site 13. Considering adjacent cores, the quartz grains usually preferentially accumulate at the high elevations.

Volcanic Ash and Sedimentation Rates

All cores in the survey area contain small percentages of volcanic shards and most have ash layers or pockets (Fig. 12). North of the sub-plateau the ash is white but to the south it is gray or brown. Within the sub-plateau, the uppermost layers are white and the lower ones grade from brown to black down the core. The angular shards indicate explosive sub-aerial volcanism; they are therefore aeolian deposits. The ash must have been injected high into the atmosphere

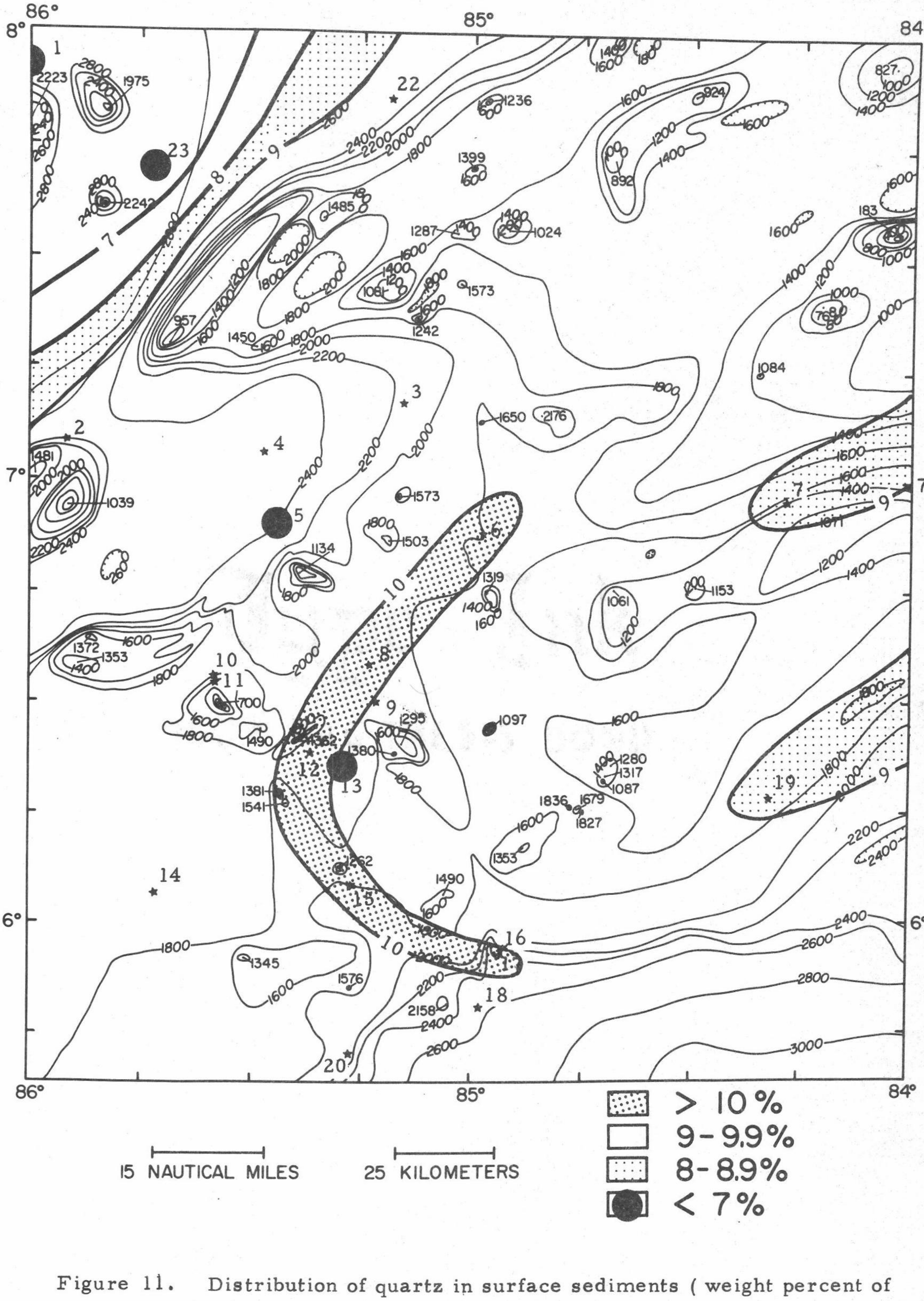

Figure 11. Distribution of quartz in surface sediments (weight percent of carbonate and opal free sediment).

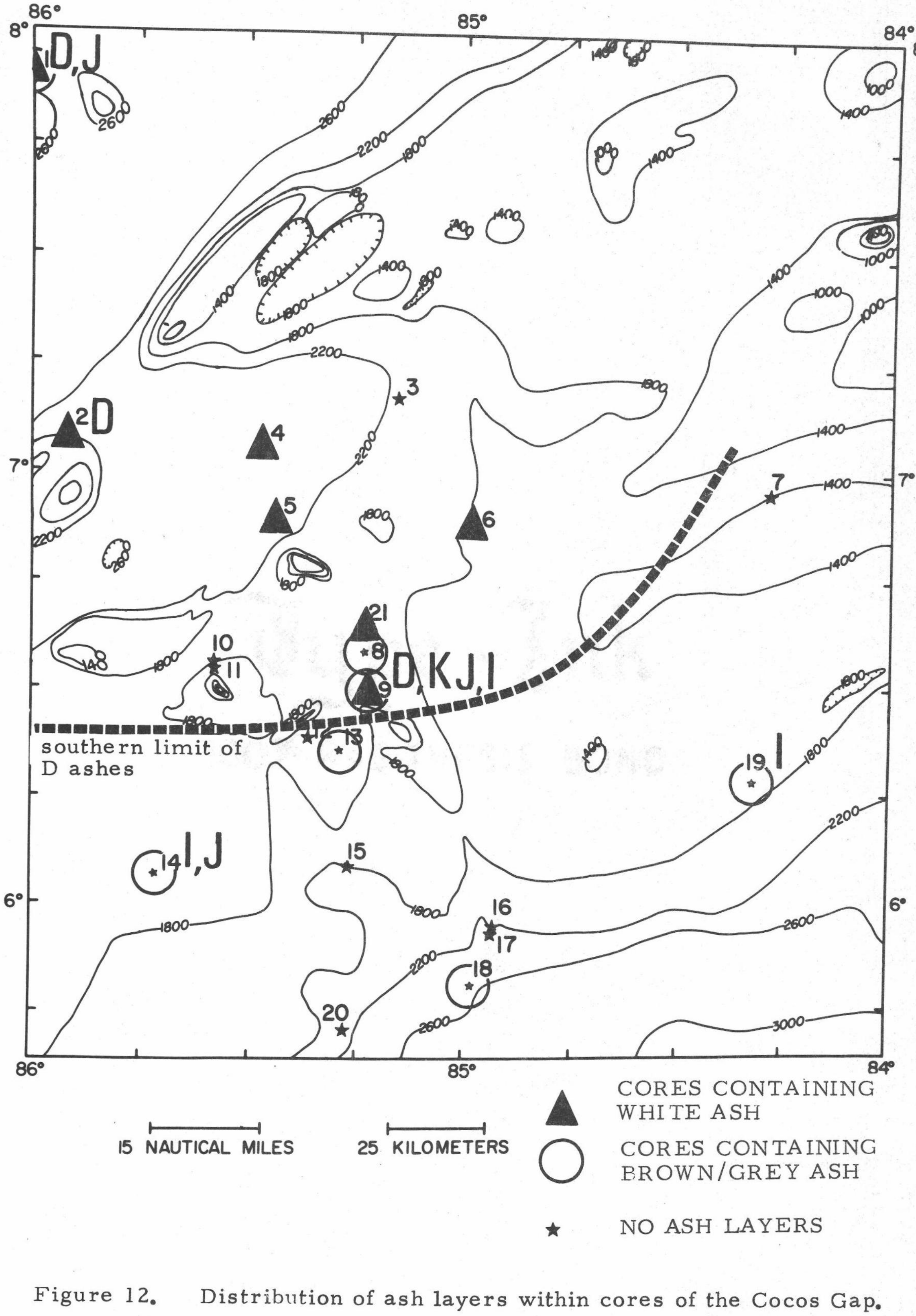

Figure 12. Distribution of ash layers within cores of the Cocos Gap. Letters indicate layers recognised by Bowles _et al._ (1973).

as easterly winds are only found in this region at heights of 1600-6000 m (U. S. Navy, 1959; Lamb, 1970), while below this height, weak westerlies predominate (Stevenson et al., 1970).

The white ash (layer D) has been attributed by Bowles et al. (1973) to the Tecpán-Chimaltenango Basin in the Guatemalan Highlands and given an age of about 54,000 years B. P. The source and age of the brown ash (layers I, J; Bowles et al., 1973) are more difficult to determine since compositionally the Cocos Ridge I and J layers are anomalous with respect to the I and J layers elsewhere in the region. Bowles suggests a tentative source for the second ashes is El Salvador or Nicaragua, with a probable age of 160,000 years B. P.

Accepting an age of 54,000 years for layer D, a sedimentation rate of 13 m/m. y. for site 9, 78 m/m. y. for site 4, and 47 m/m. y. for site 5 can be estimated. At DSDP Site 158 the late Quaternary rate is 28 m/m. y. (Heath and van Andel, 1973). These extreme local variations indicate the importance of near-bottom transport and deposition.

The distribution of ash layers is highly variable; adjacent cores show great variety in thickness of the layers (0-17 cm) and certain layers may be absent. This suggests that after the ash has reached the area it is relocated by bottom currents and accumulates as a lag deposit. Within the main channel the thicker and more numerous ash layers at site 5 compared to sites 3 and 4 indicate that this locality is particularly susceptable to lateral reworking.

The white ash (layer D) probably enters the area from the north or northeast from Guatemala (Bowles et al., 1973) while the brown ash (layers K, J) enters from the southeast or northeast (Fig. 12). The distribution within the Cocos Gap indicates a more southern source than El Salvador or Nicaragua, probably Costa Rica since Panama has been volcanically inactive throughout the Quaternary (Terry, 1956).

Texture of the Sediments

The sediments of the Cocos Gap were hydrodynamically separated into three size fraction (coarse or sand-sized, > 63 micron; silt-sized, 2-63 micron; fine- or clay-sized, < 2 micron). The coarse fraction (Fig. 13a), which mainly consists of planktonic foraminifera, is concentrated on the plateau crest, with moderate values extending into the northern part of the plateau and to site 17. The silt-sized fraction, which includes carbonate, siliceous and terrigenous components, is concentrated on the sub-plateau and northeast part of the ridge (Fig. 13b). The fine fraction, predominately non-calcareous, is restricted to the main channel, abyssal depths and southern flanks of the ridge (Fig. 13c). The areas of concentration of the three fractions are to a large extent mutually exclusive, and this is enhanced by the mathematical restraint imposed on the data by the

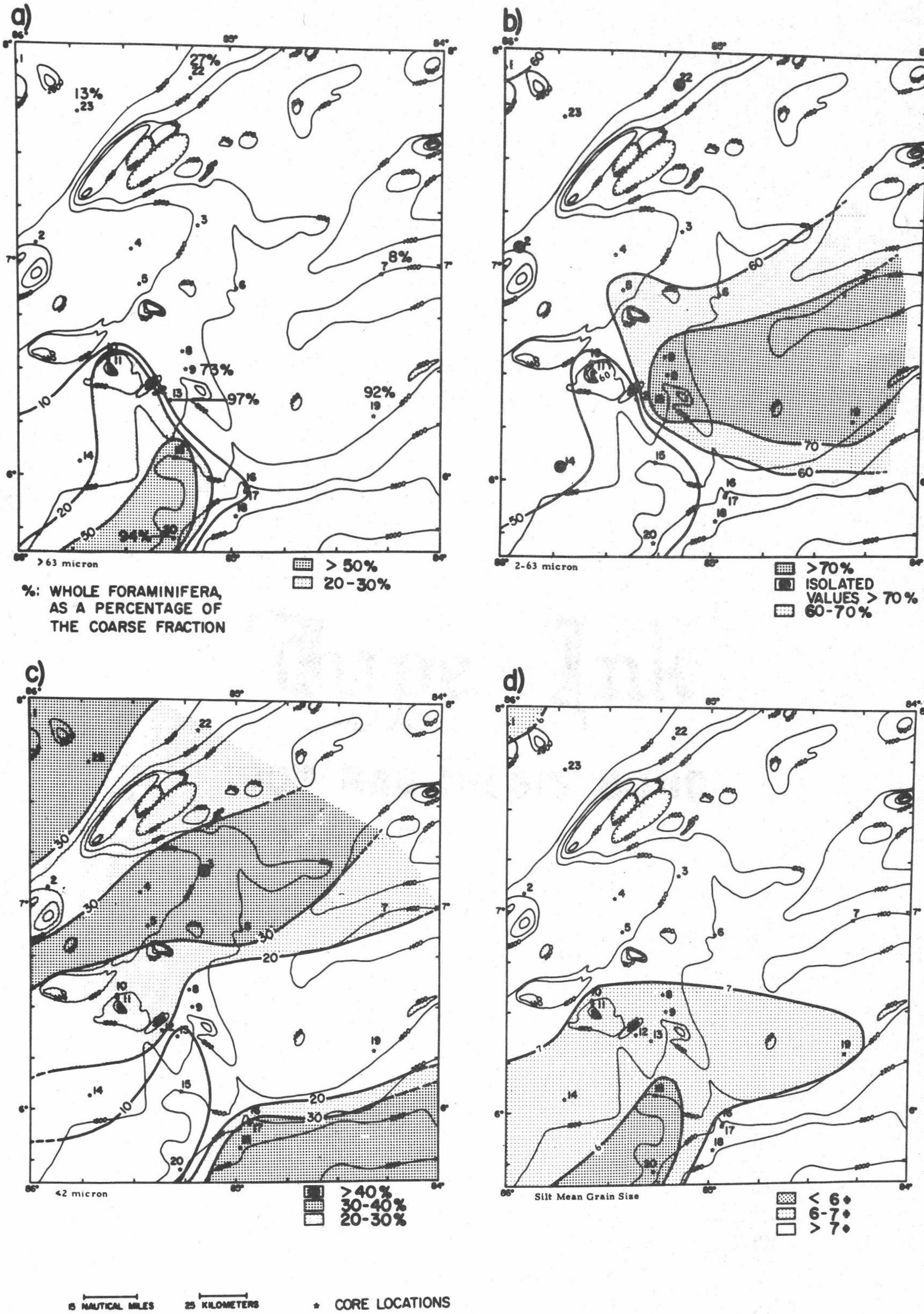

Figure 13. Distributions of the grain size fractions: a) >63 micron b) 2-63 micron c) <2 micron (weight percent of total sediment). d) mean size of silt size fraction (in phi).

condition that the sum of the variables is constant (Chayes, 1960).

Textural analysis has often been useful as a tool in tracing sediment dispersal paths, particularly where areal distributions of the individual components of polymodal sediment are available (Curray, 1960; van Andel, 1973). For the Cocos Gap the silt-sized fractions of 20 cores were hydrodynamically separated, and size distributions determined with a settling tube (the Cahn Electrobalance). The technique was described by Oser (1972) and Dauphin (1972). The silt-sized fraction was chosen for the study as it is the most compositionally varied fraction, has at least two principle sources and is more mobile than the coarse fraction. The various components of the polymodal size distribution are grouped into three classes (A1-2, B1-3, C1-3, Fig. 14), and these correspond well with those described by van Andel (197) for the Panama Basin as a whole. Proportions of the modes (Table II) are expressed as weight percentages of the silt-sized fraction rather than as percent of the total sediment to avoid the dominating influence of the other size fractions. The coarsest silts occur on the plateau (Fig. 13d), from where they grade east and northward to fine silts in the main channel and along the southern flanks of the ridge (see Appendix for sample preparation).

The distribution of the A modes (Fig. 15a, b) is similar to that of the carbonate (Fig. 8b) and coarse fraction (Fig. 13a) (correlation coefficients: 0.58 and 0.59, respectively). This is in accordance

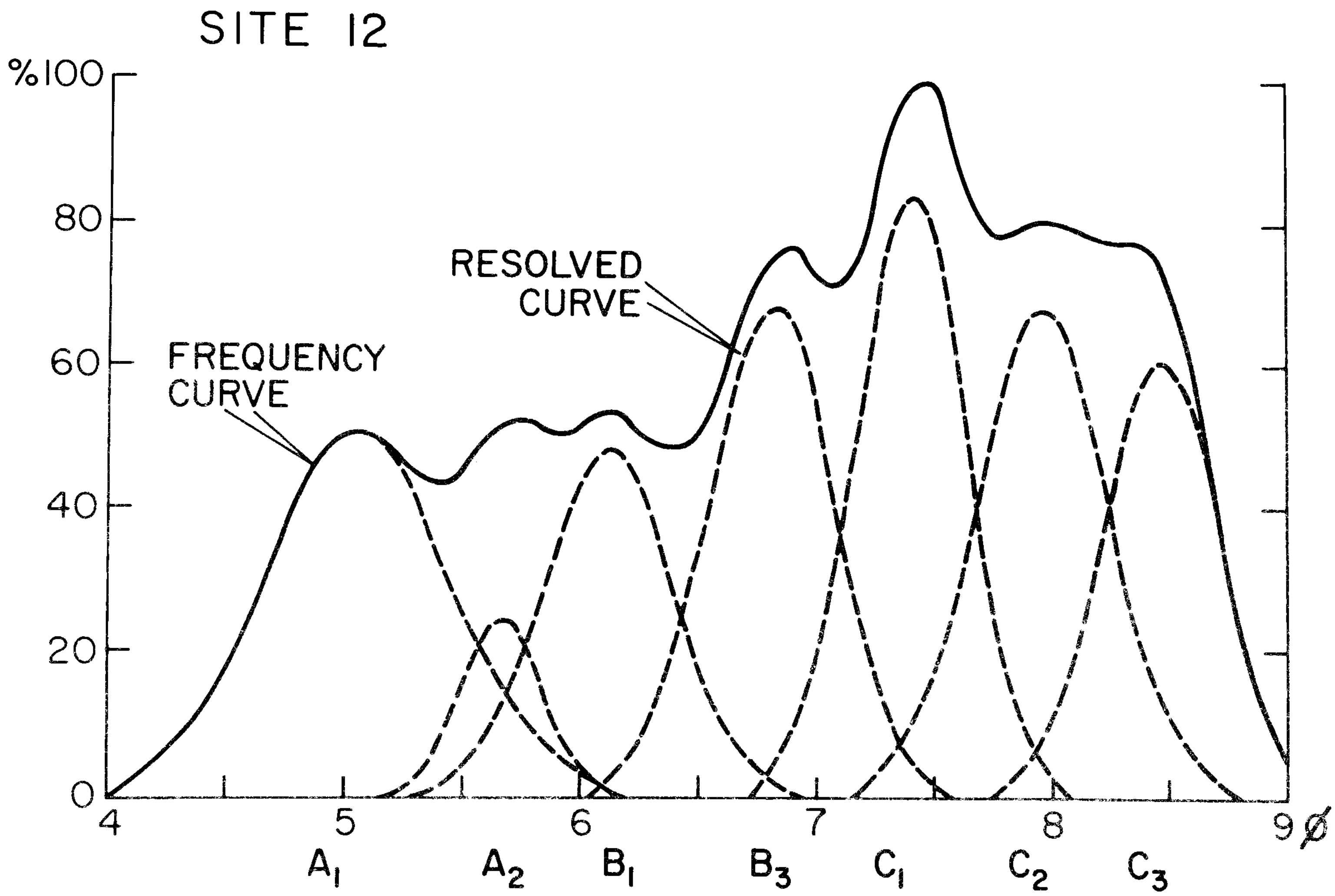

Figure 14. An example of a size frequency distribution and its component modes. Letters indicate modes mentioned in the text.

TABLE II. Sample Textural Data.

Core No.	> 63 μ	2-63 μ	< 2 μ	Mean Silt Grain Size	Silt Mode Data							
					A_1	A_2	B_1	B_2	B_3	C_1	C_2	C_3
1	0.2	68.0	32.8	6.6	28	0	9	6	23	8	21	5
2	0.2	74.4	25.4	7.0	0	21	0	17	13	0	40	9
3	4.2	50.8	45.0	7.3	1	15	0	5	18	23	24	17
4	3.6	58.2	38.2	7.2	12	0	10	4	7	45	2	20
5	2.6	67.2	30.2	7.2	0	17	1	0	23	13	44	2
6	3.9	62.0	34.1	7.1	14	0	0	15	6	32	15	18
7	0.5	74.0	25.5	7.0	0	13	8	0	27	21	14	7
8	3.2	80.6	16.2	6.8	16	8	8	0	26	17	20	5
9	9.4	79.7	10.9	6.5	23	3	11	10	21	4	21	7
10	26.0	46.9	27.1	6.7	25	2	9	0	11	34	6	13
11	29.7	50.1	20.2	6.5	42	0	3	9	0	15	18	13
12	27.3	48.0	24.7	6.8	19	5	12	0	16	18	17	13
13	9.0	84.4	6.6	6.3	31	13	0	0	28	16	10	2
14	13.5	76.2	10.3	6.7	22	0	13	10	15	18	20	2
15	51.5	45.7	2.8	5.9	46	10	0	17	4	14	3	6
16	7.8	56.7	36.5	7.0	0	26	3	0	12	22	28	9
17	10.9	52.9	36.2	7.1	14	1	0	20	1	22	18	24
18	6.7	53.4	39.9	6.9	2	21	0	8	14	9	32	13
19	1.7	81.5	16.8	6.5	26	8	1	0	32	4	21	8
20	52.8	45.7	1.5	5.9	50	5	22	0	8	7	6	2
21												
22	1.7	77.6	20.7									
23	1.2	48.5	50.3									

Figure 15. Distributions of the silt-size modes: a) A1, b) A2, c) B2, d) B3, e) C1, f) C2. (weight percent of silt-size fraction)

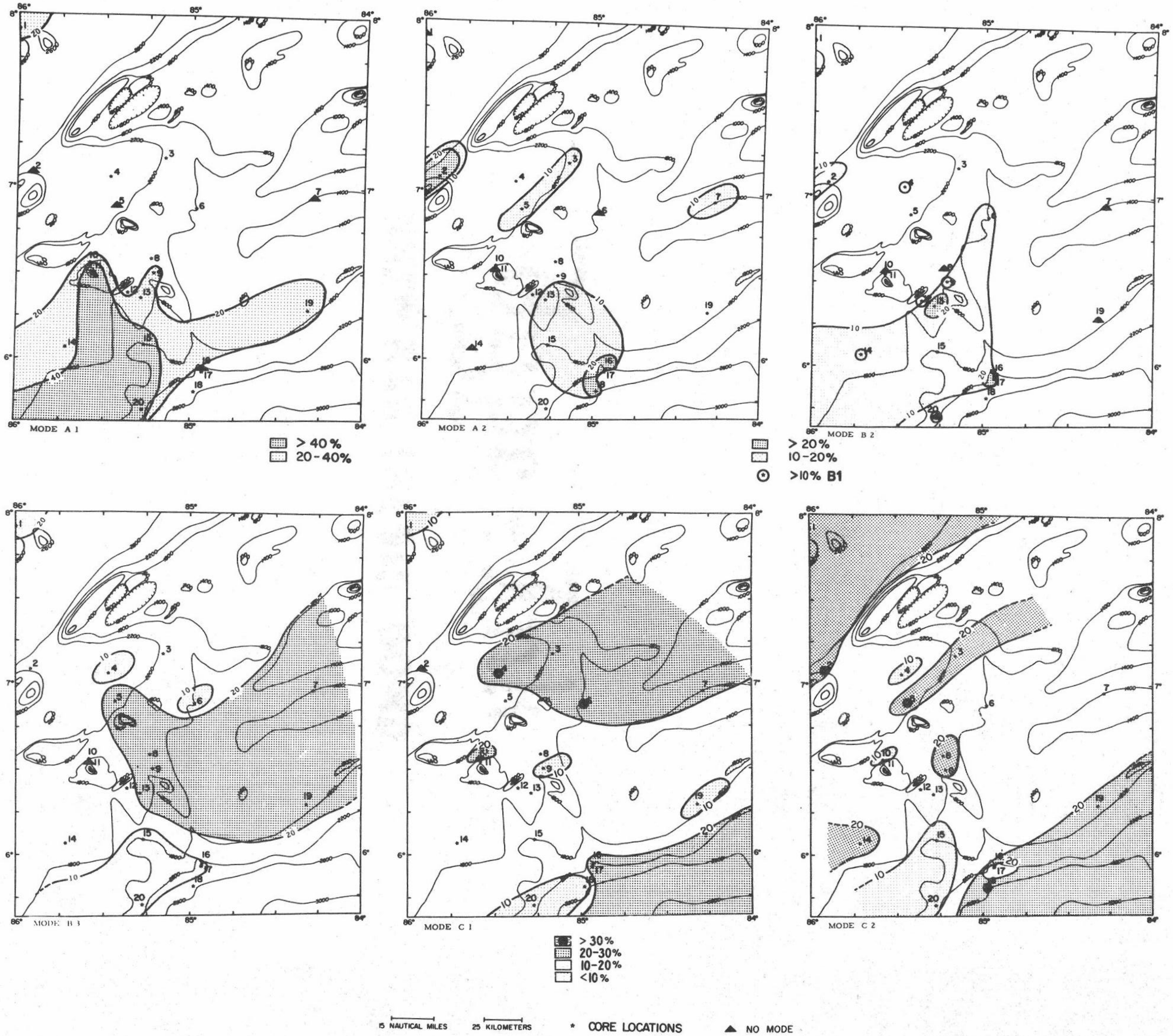
MODE A 1
> 40%
20-40%
MODE A 2
MODE B 2
> 20%
10-20%
>10% B1
MODE B 3
MODE C 1
MODE C 2
> 30%
20-30%
10-20%
<10%
15 NAUTICAL MILES
25 KILOMETERS
CORE LOCATIONS
NO MODE

with the observation at site 11 that these modes consist of 98% foraminiferal fragments. The high values of A1 correspond to the plateau and there is a uniform reduction of percentages away from here, with a prominent lobe of material extending from basin C downslope into basin B. Mode A2 is a secondary mode generally only present when A1 is absent, with low values and a more scattered distribution (Fig. 15b). The most significant A2 distributional features are the higher values on the east of the plateau, downslope from the plateau crest (sites 16, 18; Fig. 15) and in the south of the main channel.

The distribution patterns of B1 and B2 are also to some degree mutually exclusive while B3 is found at all sites except 11. B1 is found astride the plateau crest and in the deepest part of the main channel while B2 is concentrated in the plateau and sub-plateau (Fig. 15c). The distribution of B3 is similar to the overall silt-size distribution (Fig. 13b) ($r^2 = 0.56$). At site 11, modes B1 and B2 consist of foraminiferal fragments (82%), clay minerals (8%), siliceous fragments (5%), and coccoliths (5%). Site 3 has foraminiferal fragments (42%), siliceous fragments (25%), and minerals (33%) for modes A2 (41%), B2 (13%), and B3 (46%) (100% : total decanted A2-B3 material). Therefore, the B modes are transitional and reflect both terrigenous and biogenic input.

The distribution of B1 suggests that it is the finest recognizable silt-sized carbonate chaff in the area while B2 is likely to be a siliceous terrigenous lag-type deposit with formainifera fragments and possibly volcanic ash. Their mutually exclusive distributions may be accentuated by the curve resolving technique used, as the percentages are small.

The C modes are concentrated in the main channel and along the southern flanks of the ridge (Fig. 15e, f). Modes C1 and C3 have an almost identical distribution pattern while C2 is more scattered. At site 3 these modes consist of 63% clay minerals, the remainder consisting of foraminiferal fragments and small percentages of coccoliths, siliceous fragments and non-clay minerals. However, away from the terrigenous influence (at site 11), about 55% of the C mode consists of coccoliths, with about 20% clay minerals and the rest of the sediments as foraminifera fragments, siliceous fragments and non-clay minerals. An equivalent Coccolithus pelagicus mode was found by Oser (1972) in northwest Pacific sediments. Therefore, the modes can only be used to delineate the sediment transport paths through an area after careful regard to the composition of the dominant mode component.

Reworked Tertiary Material

Most of the cores include reworked Tertiary material and four Tertiary sources associated with large scale faulting were recognized

(Fig. 16). At the head of basin A, major faults expose older sediment (Fig. 3) which is probably the source of the Upper Miocene radiolarian assemblage found downslope at site 6 (Fig. 16). In the main channel, no Miocene fossils are found at site 3, but an admixed Pliocene radiolarian assemblage is found at sites 3 and 4, admixed Pliocene material also occurs in basin A (T. C. Moore, Jr., personal communication). Therefore, Pliocene sediment is probably exposed along the fault controlled flanks of the channel near both sites and also at the head of basin A.

On the south flank of the ridge Miocene sediment is probably exposed by faults, as an almost complete Middle Miocene radiolarian assemblage is found at site 16 (T. C. Moore, Jr., personal communication) (Fig. 16), immediately to the south of prominent faults (Fig. 7b). Miocene material, either slumped or wafted downslope by bottom currents (Moore, 1970) from near site 16, is found at sites 17 and 18. Other Tertiary sources, especially associated with faulting in the plateau, certainly occur but are not clearly identifiable.

The dispersal pattern suggests entrainment in southwestward flowing bottom water supporting the flow pattern postulated earlier. It also indicates that the flow into basin A is separate from that of the main channel.

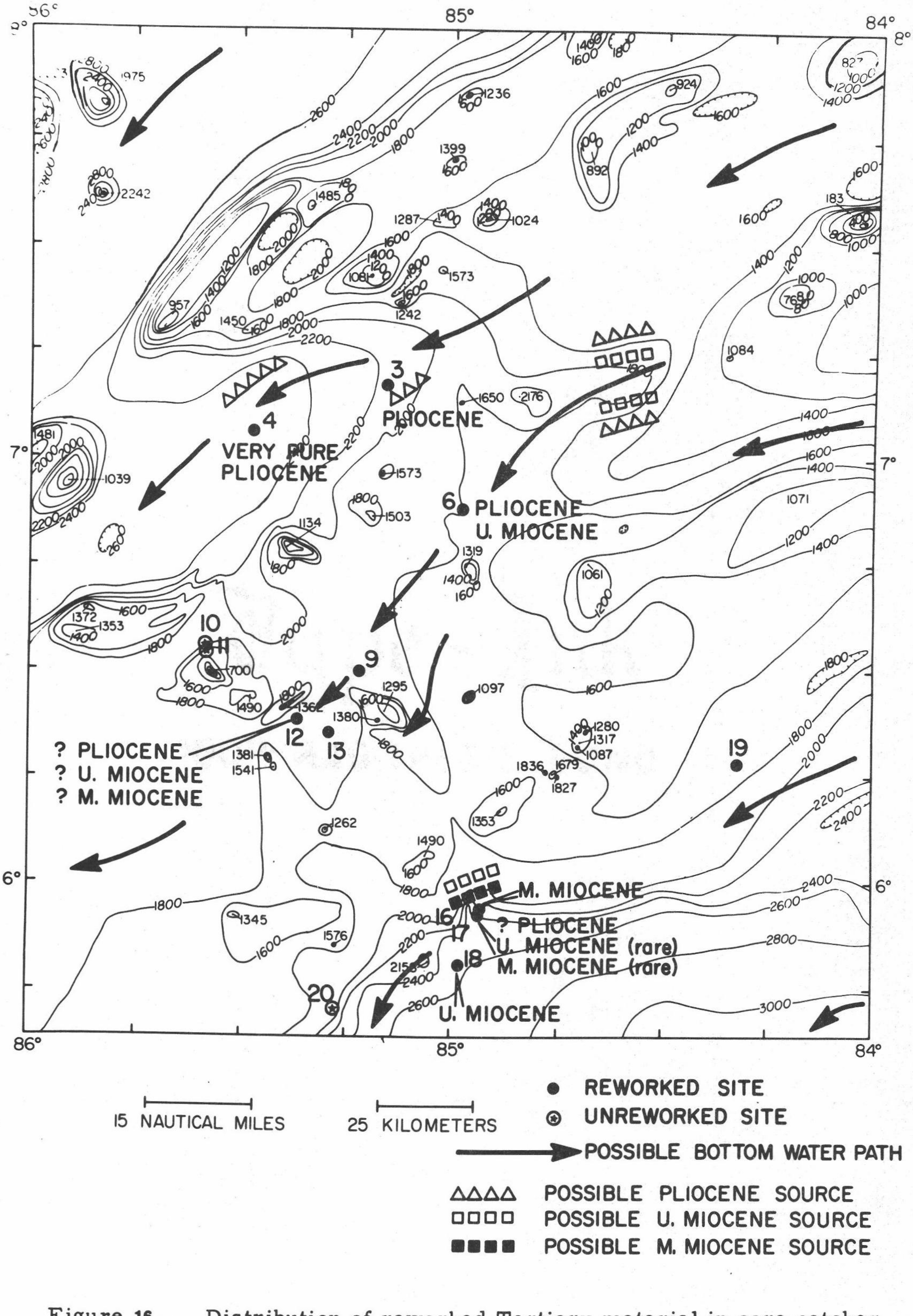

Figure 16. Distribution of reworked Tertiary material in core catcher samples. Possible Tertiary sources and bottom water flow pattern marked.

DEPOSITIONAL PROCESSES IN THE COCOS GAP

The sediments of the Cocos Gap consist of four main components: biogenic calcium carbonate, silica, terrigenous clay and quartz. Minor components include volcanic ash and authigenic clays. Of these, the first two are mainly produced in the euphotic zone, while the latter, excluding the authigenic clays, are carried in by wind and by near bottom currents.

The Cocos Gap lies southeast of the Costa Rica Dome and at any given time the productivity gradient varies from northwest to southeast (600 to 200 $mgC/m^2/day$; Moore et al., 1973). The Dome, however, migrates seasonally, and the net long term input of biogenic material is probably uniform over the Cocos Gap. The terrigenous and volcanic inputs, on the other hand, are likely to have well defined dispersal paths and gradients.

Superimposed on this pattern of sources and transportation paths are local processes (increased carbonate dissolution associated with depth; winnowing of material at shallow locations and downslope dispersal of the fine fraction; and reworking, transport and erosion by bottom currents on both local and more regional scales, aided by the effects of bioturbation). The compositional and textural data presented above can be interpreted to provide some insight into the relative importance and effects of these processes.

Sedimentary and faunal evidence indicates that bottom water flows southwestwards through the area (Fig. 16), its pattern locally controlled by topography. The distribution of the clay-size fraction (Fig. 13c) suggests that the fine terrigenous material is incorporated into this flow, enters the area at three localities and follows three separate southwestward dispersal paths: through the northern abyssal depths, along the main channel and along the southern flanks of the ridge. The distribution of the Tertiary material (Fig. 16) indicates that the bottom water flow into basin A, and its associated sediments, is separate from the flow down the main channel (Fig. 16).

The detritus grain size data and microscopic analysis of the silt-size modes suggests that the terrigenous input down the main channel is recognizable in both the silt and clay size fractions (< 63 micron). Therefore, it must have a nearby source, possibly Costa Rica. Along the southern flanks, the terrigenous input is only recognizable in the C mode and clay-size fraction (< 8 micron), suggesting a distal deposit from the large scale circulation of the Panama Basin, with a source in Colombia or Ecuador (Heath et al., 1974).

The distribution of the coarse terrigenous material (B3, silt: Figs. 15d, 13b) reflects an influx of minerals or coarse clay aggregates from Costa Rica along the ridge crest (Fig. 17). It passes into the sub-plateau but not along the plateau crest, and the low value of B3 in basin A suggests that the sediment settles in the ridge crest

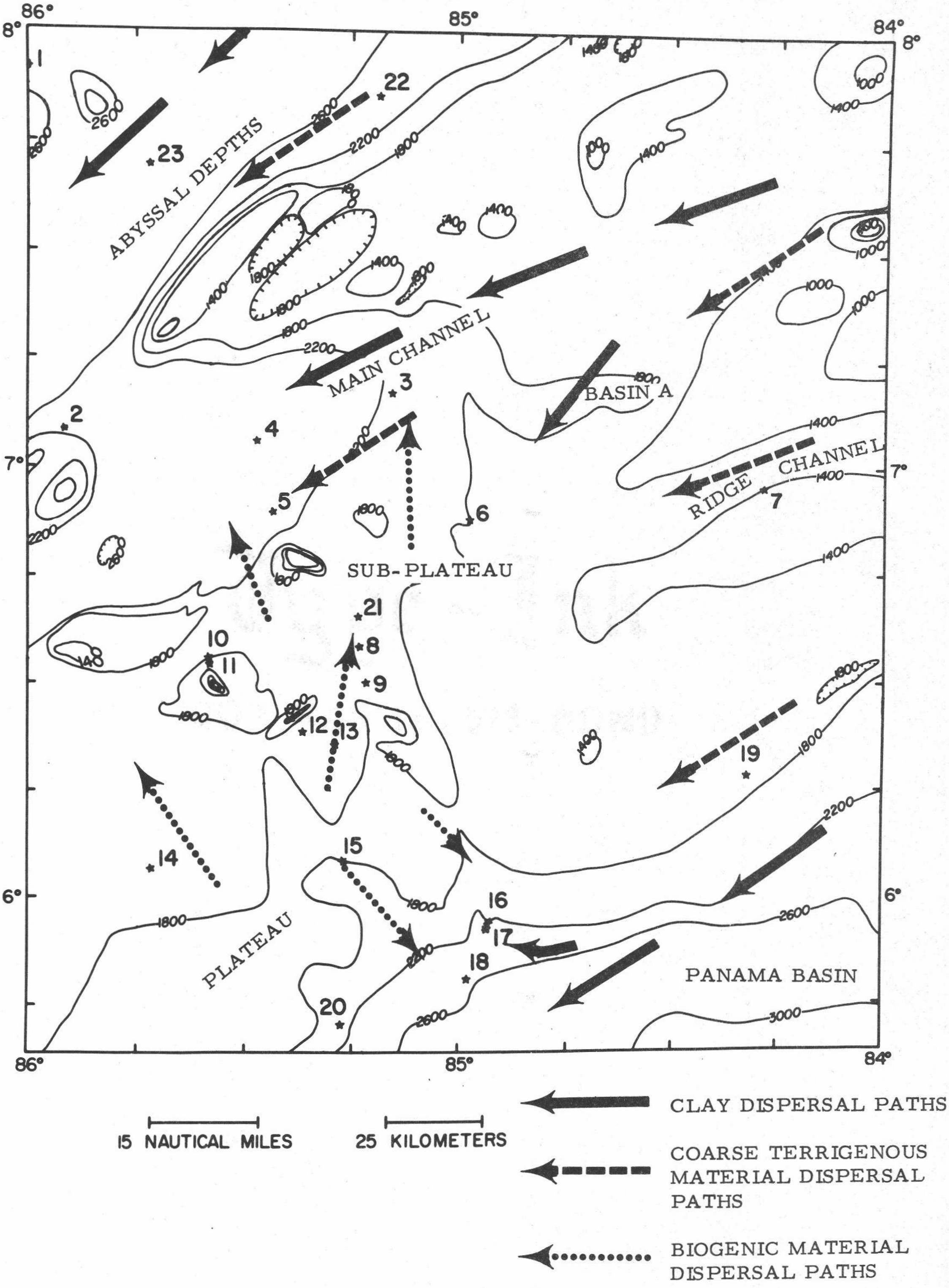

Figure 17. Sediment dispersal paths within the Cocos Gap area.

and does not reach this basin. The inclusion of sites 7 and 19 into the patterns suggests that the transportation mechanism may be upper flank contour currents. These probably result in the more scattered distribution of C2 (Fig. 15e) compared to the clays (Fig. 13c) or organic carbon (Table I), and its preferential accumulation at site 5 rather than sites 3 or 4 in the main channel. More ash layers have accumulated at site 5 than at sites 3 or 4, indicating that the shards may be lag deposits of the upper flank contour currents. Therefore, the postulated transport of modes by the upper and lower contour currents may be reflected in compositional variations, with the former associated with more lag-type deposits.

The biogenic components are diluted by clays associated with the bottom currents, especially in the main channel, as the lowest carbonate values are found here (Fig. 8a). Similarly, the shallow carbonate group III sites (Fig. 8b) reflect dilution by terrigenous material entering the area via the ridge channel. The similarity between the carbonate values at flank sites (below 2000 m) suggests that in the south, dissolution masks dilution by clays associated with the lower contour current. Organic carbon values (Table I) correspond to the clay values and indicate areas of terrigenous dilution (with > 3% organic carbon). The plateau is largely unaffected by the influence of terrigenous material, but the small amount that does enter does so via sites 9 and 12 rather than the more elevated route (sites 9 and 13) favored by the descending biogenic components.

The high opal values for the southern sites compared to the northern flank (Fig. 9) suggests that either the southern sites are influenced by a greater influx of opaline chaff from the ridge crest than the northern sites or that the opal distribution is intimately associated with the lower contour current. The high opal sites are above the opaline chaff zone (Moore et al., 1973), and the lower contour current, passing across the opal-rich chaff zone, may resuspend opaline fragments which then settle upslope. Similarly, bottom currents entering the main channel and basin A carry resuspended chaff from the ridge crest. The factors controlling this redeposition may be a function of the roughness or slope of the local sea floor, benthic activity or a reduction in bottom current velocity at a particular locality.

Assuming uniform input for carbonate, opal and quartz, the variations in the relative proportions of these components and their modal distributions are a function of winnowing efficiency superimposed on the size sorting of the particles during their lateral relocation by bottom currents. In addition, the carbonate fraction is subjected to depth related dissolution, including corrosion of the foraminifera, dissolution of fine particles and reduction in the total carbonate content of the sediment. The end products of winnowing and dissolution are very similar, therefore, as dissolution effects are more regional, they will be considered first.

Anomalously low carbonate values were found in the region compared to equivalent positions elsewhere in the Panama Basin (Moore et al., 1973). This suggests that the northern part of the Cocos Ridge is an extremely harsh environment for foraminifera. The controlling factor is probably the position of the Lysocline. Luz and Shackleton (1975) have shown that the total amount of carbonate preserved in the sediments below the Lysocline is a function of dissolution, whereas near to this zone, although dissolution is intense, the amount preserved is largely unaffected by fluctuations in solution intensity. Within the Cocos Gap, the critical depth is about 2000 m (500 m below the Lysocline) as above this depth the carbonate values vary from 35-75% but below it the values are less than 20% (Fig. 8b). The regional rise of Lysocline towards the continent (Lisitsin, 1971, 1972; Berger and Winterer, 1974) is not significant as all but two of the sites are in a 50 km band parallel to the coast and 325 km offshore.

Since above 2000 m the total amount of carbonate preserved is largely independent of dissolution within this small area the major controll on carbonate is downslope winnowing. Therefore, the dominating dispersal mechanism within the Cocos Gap is probably mechanical breakdown of corroded foraminifera and mechanical or biological resuspension. Subsequently, the fragments (including the fine non-carbonate fraction) may be transported downslope as dilute suspensions under the influence of gravity or transported laterally by bottom currents (Fig. 17), leaving behind a lag deposit of resistant foraminifera, minerals, volcanic glass and quartz grains.

As the depth difference between the plateau and sub-plateau is only about 100 m and masking by clay dilutants is negligible in these areas, the comparatively low coarse fraction values (Fig. 13a) but high carbonate values (Fig. 8a) suggest that in the sub-plateau the foraminifera are most subjected to mechanical breakdown. This is supported by the general fragmentation of the biogenic fraction and the small number of whole foraminifera and radiolaria in the coarse fraction. Silt-size modal analysis indicates that the coccolith carbonate contribution is very small. In addition, the sub-plateau is more efficiently winnowed than the plateau (possibly because it has a more steeply slope sea floor) as shown by the absence of transitional silt-size modes, the relatively low carbonate mode percentages (A1-B1) and the low carbonate-free opal values in the area; the particularly low carbonate value at site 8 may indicate where removal has been most thorough.

Therefore, the sub-plateau is the most transitional environment and is probably the source area for the fine biogenic material in the main channel. A comparison of the carbonate silt-size modes suggests that some of the material (A1) wafts downslope from basin C to basin B (site 13 to 9), probably under the influence of gravity. Here it is further corroded, broken, winnowed and then transported with the indigenous fragments to the southern flanks of the main channel (A2) and finally to the deeper parts of the channel or to isolated pockets (B1) (Fig. 17). Yamashiro (1975) recognized a high "in transit" foraminiferal assemblage for this area. Conversely, the moderately high A1 and A2 values on the plateau and the pockets of B1 astride the crest (Fig. 15c) suggest that there is limited net loss of silt-size sediment from the plateau.

The extreme reduction of foraminifera to silt-size fragments is likely to be associated with the suspected tidally induced intensification of bottom water flow. Sedimentary data indicates that the process is probably most significant in the sub-plateau. This breakage to silt-size fragments accounts for the anomalously low percentages of foraminiferal fragments found in the coarse fraction of the northern part of the Cocos Ridge by Kowsmann (1973). On the plateau, the bottom water flow is probably predominately tidally induced cyclical flow, not associated with significant downslope winnowing. Lonsdale et al. (1972) reported upslope migration of bed material in response to tidal currents on the Horizon Guyot and a similar response here could accentuate the lag accumulations such as quartz.

During the dispersal process, the radiolaria are easily broken; when intact, they preferentially settle on the foot of ridge slopes (Moore et al., 1973) above the opaline chaff accumulations.

Therefore, they are good winnowing indicators. There is selective accumulation of silica within the ridge, for example, siliceous fragments are winnowed from the crest and carried to the ridge channel where the radiolaria settle while the lighter material is transported further downslope to the radiolaria-poor, opal-rich basin A (Fig. 9). Further winnowing into the main channel is likely. The generally small percentage of diatoms present indicates that the lightest material is completely removed from the area.

There is transport of sediment into the Panama Basin across the Cocos Gap, particularly the coarse fraction, silt-size quartz grains, siliceous fragments and minerals to site 17 and fine carbonate material (A2) to the adjacent sites 16 and 18. Localized channeling and slumping associated with the oscillating tidal flow across the Gap are the most probable mechanisms since core descriptions indicate that turbidity flow is not significant. Similar downslope transport of sediment from the sub-plateau to the main channel is probable, as indicated by the high A2, B3 and moderate total silt-size values at site 5. Low opal and very low quartz values here indicate dilution by the winnowed material.

Environments within the Gap are significantly different from those on the flanks of the ridge. For example, site 20 (1838 m) and site 19 (1734 m), about 120 km apart, are at equivalent depths, but the site on the crest of the Gap (20) has no reworked material and significantly more carbonate and coarse fraction than the flank site. Conversely, the flank site has relatively more fine carbonate (< 63 micron) but coarse (A1) rather than fine chaff predominate as the clay size fragments accumulate further downslope. Apparently, the upper flanks of the ridge are more susceptible to slumping, reworking and winnowing by directional bottom currents (contour currents) while the flatter saddles are dominated by tidally induced cyclical flow. The saddles thus act as biogenic catchment areas.

Bioturbation plays an important role in the vertical and lateral transport of sediment through the area, as burrowed muds are more easily resuspended than those that are not (Rhoads, 1970; Rhoads and Young, 1970). In addition, worm burrows decrease the shear strength of clay (Richards, 1965) so that slumping may be initiated. This is probably most critical on the seamount and main channel walls, especially where the numerous Tertiary outcrops are exposed by faults. Texturally, burrowing is important as the hydrodynamic properties of the sediment are altered by benthic organisms, particularly by passage through the gut of the animal and the formation of fecal pellets. Selective sorting of the sediment by the organism occurs on a very local scale.

CONCLUSIONS

The Cocos Gap is a deeper portion of the Cocos Ridge that is probably typical of saddles within most shallow oceanic ridges. Sedimentation within it is controlled by local processes rather than by the broad regional ones of productivity in the euphotic zone, regional dissolution or the thermohaline circulation system. Hydrographic data indicates that there is no significant transport of water either into or out of the Panama Basin across the Gap, but that the only flow recongizable from these parameters is parallel to the main trend of the ridge.

Sedimentary data indicates that bottom water flows southwestwards through the Cocos Gap and is predominately controlled by topography. Localized areas with small channels and sediment mounds indicate that the directional pattern has dendritic characteristics as it follows a network of depressions. A postulated contour current which is part of the circulation of the deep water of the Panama Basin is found along the southern flanks of the ridge. Flow of intermediate water along the ridge occurs as postulated upper contour currents along both ridge flanks and as flow along the crest of the ridge. Surface water flow is variable, mainly because of the seasonal mobility of the dominant hydrographic feature, the Costa Rica Dome, associated with the migrations of the Inter-Tropical Convergence Zone.

The sediments of the Cocos Gap are predominately olive grey calcareous oozes, dominated by planktonic foraminifera on the plateau and by clays at increasing depths. Selective sedimentation, non-deposition and scouring by bottom currents occurs, as shown by areas of barren basement and by moated seamounts with adjacent sediment accumulations. However, there is no evidence for selective sedimentation to the lee side of the hills. The basins found here are infillings of basement grabens and their surfaces are remarkably level.

Sedimentation rates are therefore a function of the distance to biogenic or terrigenous sediment sources, of relocation by bottom currents, and of entrapment in grabens of the fractured basement. Consequently, they vary considerably as deduced from ash layer ages (site 4: 78 m/m.y.; site 5: 47 m/m.y.; site 9: 13 m/m.y.) and biostratigraphy (site 21 - DSDP Site 158: 28 m/m.y., Heath and van Andel, 1973). The angular nature of the shards, varying layer thicknesses and sporadic distributions indicate that the ash layers are lag deposits of aeolian origin that were relocated by bottom currents (particularly the postulated upper contour current) after entering the water column and moving with the intermediate waters.

The Cocos Gap is divided into six morphologically distinct regions, each with its own sedimentation characteristics. The abyssal depths are part of the Guatemala Basin and terminate in the south abruptly at the northern flanks of the ridge. The crest of the ridge is separate from a northern range of seamounts by the most prominent topographic feature, the main channel. In the northeast, the main channel is separated by basement ridges and major faults from a deep depression, basin A, that forms the southern part of the sub-plateau, a gently sloping area adjacent to the plateau, or crest of the Cocos Gap. To the west and east of the sub-plateau and plateau, the Cocos Ridge rises steeply, with one prominent channel (the ridge channel) to the east of basin A.

In order to determine the mechanisms controlling sediment dispersal, the nature and sources of the sediments were defined. A textural study indicates that the coarser material (> 63 micron), consisting of planktonic foraminifera, is preserved mainly in the plateau while the silt-size fraction (2-63 micron) consists predominantly of foraminiferal and siliceous fragments winnowed from the plateau and sub-plateau, and minerals from Costs Rica transported along the crest of the ridge associated with postulated upper contour currents. The clay-size fraction (< 2 micron) is amorphous material with very low percentages of well crystallized clays. Apart from the authigenic clays that have a ridge crest source, they have three sources and transport paths: fine material that is transported through the abyssal depths, possibly with a Central American source, coarse clays from Costa Rica that occur in the main channel, and fine material from

Colombia or Ecuador that is carried by the postulated lower contour current. The clays reaching sites 16, 17 and 18 probably settle away from the main flow of the contour current, and are associated with the general circulation within the Panama Basin.

The most compositionally varied fraction, the silts, have eight textural modes in three classes (A1-2, B1-3, C1-3). Modes A1-B1 reflect the progressive breakage and winnowing of the coarse fraction under the influence of bottom currents and gravity. The B modes in general represent transitional facies, with both biogenic and terrigenous influences, while the C modes characterize the clay mineral regimes.

The principal mechanism controlling the carbonate distribution below 2000 m is dissolution, as dilution is only significant in the main channel, basin A and the ridge channel. Above this depth, mechanical breakdown of corroded foraminifera predominates. The fragments are resuspended and dispersed downslope or laterally by bottom currents. Biogenic resuspension by burrowing or respiratory movements is probably important as burrowing is common, two morphologies particularly being preserved. Associated with the burrowing are slumping, selective sorting of sediments by the organism and the alteration of hydrodynamic properties of the sediment.

The crest of the Gap acts as a catchment area for biogenic components, while the more sloping sub-plateau is the carbonate and opal source area for the deeper parts. The finest, clay-size material is efficiently winnowed from the area. The extreme breakage of the foraminifera is a function of the tidally induced intensification of bottom water, characteristic of many shallow oceanic areas, and is most significant in the sub-plateau.

Transport of sediment into the Panama Basin is associated with cyclical tidal reversals of the bottom water and sediment slumping as coarser carbonate, siliceous fragments and minerals (coarse fraction, quartz, B2, B3) collect at site 17 and the finer carbonate (A2) at the adjacent sites 16 and 18.

Along the southern flanks of the ridge, slumping, reworking and winnowing by downslope displacement under the influence of gravity and by postulated upper flank contour currents results in the accumulation of fine carbonates and opal along the lower flanks of the ridge and the coarser carbonate fragments remain behind as part of the lag deposits. Within the Cocos Gap, the lag deposits are mainly resistant foraminifera, quartz grains, minerals and volcanic shards. Radiolaria concentrate in intermediate positions and in sheltered basins. The high opal values along the southern flanks of the ridge suggest that the postulated lower contour currents may introduce resuspended opal into the area. This may be a function of the roughness of the local sea floor, benthic activity or a reduction in bottom current velocity at a particular locality. The main channel is similarly affected, but the lower less uniform values (Fig. 9b) along the northern flanks indicates that this process is only significant where directional currents flow along the opal-rich zone. In general, the siliceous fragments concentrate in the transitional B modes.

The B3-C3 modes and clay-size distribution indicate that the terrigenous material can be divided into coarser (B3, C2) and finer (C1, C3, clay-size) components. These are hydrodynamically distinct and the former are transported along the more elevated ridge slopes while the latter are found at deeper sites, associated with the directional bottom water paths.

Within the more elevated areas, the absence of the clay mineral modes results in the dominance of a coccolith counterpart. Therefore, the composition of the modes is not necessarily uniform from region to region. The coccolith mode corresponds to one described for the northwest Pacific by Oser (1972), and the modes in general agree with those found in the Panama Basin (van Andel, 1973); therefore, certain absolute, as well as local, characteristics of the sediment may be recognized from modal analysis.

The combined approach of sediment textural and compositional analysis within a small well-defined area is an important link between sedimentation processes occurring regionally and at the sediment/water interface. At this level, the interaction between tidally intensified flow and directional (thermohaline) flow over a variably sloping sea floor and the nature and proportion of sediment influx, are the controlling factors in the nature of the sediments preserved. Superimposed on this is the dissolution of the carbonate fraction but at the scale of the Cocos Gap, relocation masks dissolution.

BIBLIOGRAPHY

Bentley, L. R., 1974, Crustal structure of the Carnegie Ridge, Panama Basin and Cocos Ridge: Master's Thesis. Honolulu, University of Hawaii, 48 p.

Berger, W. H., 1968, Planktonic foraminifera: selective solution and the paleoclimatic interpretation: Deep-Sea Res., v. 15, p. 31-43.

Berger, W. H., 1970, Planktonic foraminifera: selective solution and the Lysocline: Mar. Geol., v. 8, p. 111-138.

Berger, W. H. and E. L. Winterer, 1974, Plate stratigraphy and the fluctuating carbonate line: Spec. Publ. Int. Assoc. Sediment., v. 1, p. 11-48.

Bowles, F. A., R. N. Jack, and I. S. E. Carmichael, 1973, Investigation of deep-sea volcanic ash layers from Equatorial Pacific cores: Geol. Soc. Am. Bull., v. 84, p. 2371-2388.

Calvert, S. E., 1966, Accumulation of diatomaceous silica in the sediments of the Gulf of California: Geol. Soc. Am. Bull., v. 77, p. 569-596.

Chayes, F., 1960, On correlation between variables of constant sum: Jour. Geophys. Res., v. 65, no. 12, p. 4185-4193.

Curray, J. R., 1960, Tracing sediment masses by grain size modes: Report: 21st session Norden, Internat. Geol. Congress. Copenhagen, 1960, p. 119-130.

Dauphin, J. P., 1972, Size distribution of chemically extracted quartz used to characterize fine-grained sediments: Master's Thesis. Corvallis, Oregon State University, 63 p.

Detrick, R. S., D. L. Williams, J. D. Mudie, and J. G. Slater, 1974, Galapagos Spreading Center: bottom water temperatures and the significance of geothermal heating: Geophys. J. R. Astr. Soc., v. 38, p. 627-637.

Donahue, J., 1971, Burrow morphologies in north-central Pacific sediments: Mar. Geol., v. M1-7.

Ellis, D. B., 1972, Holocene sediments of the South Atlantic Ocean: the calcite compensation depth and concentrations of calcite, opal, and quartz: Master's Thesis. Corvallis, Oregon State University, 77 p.

Goldberg, E. D., 1958, Determination of opal in marine sediments: Jour. Mar. Res., v. 17, p. 178-182.

Heath, G. R., 1975, Processes controlling siliceous biogeneous deposits: In Riedel, W. R. and T. Saito (eds.), Marine Plankton and Sediments, American Museum of Natural History, New York (in press).

Heath, G. R. and C. Culberson, 1970, Calcite: degree of saturation, rate of dissolution and the compensation depth in the deep oceans: Geol. Soc. Am. Bull., v. 81, p. 3157-3160.

Heath, G. R., T. C. Moore, Jr., and G. L. Roberts, 1974, Mineralogy of the surface sediments from the Panama Basin, Eastern Equatorial Pacific: Jour. Geol., v. 82, p. 145-161.

Heath, G. R. and Tj. H. van Andel, 1973, Tectonics and sedimentation in the Panama Basin: Geologic results of Leg 16, Deep Sea Drilling Project: In Initial Reports of the Deep Sea Drilling Project, Washington, D. C. (U. S. Government Printing Office), v. 16, p. 899-913.

Heezen, B. C., C. D. Hollister, and W. F. Ruddiman, 1966, Shaping of the continental rise by deep geostrophic contour currents: Science, v. 152, p. 502-508.

Isaacs, J. D., J. L. Reid, G. B. Schick, and R. A. Schwartzlose, 1966, Near bottom currents measured in 4 km depth off the Baja California coasts: Jour. Geophys. Res., v. 71, p. 4297-4303.

Johnson, D. A. and T. C. Johnson, 1970, Sediment redistribution by bottom currents in the central Pacific: Deep-Sea Res., v. 17, p. 157-169.

Kowsmann, R. O., 1973, Coarse components in surface sediments of the Panama Basin, Eastern Equatorial Pacific: Jour. Geol., v. 81, p. 473-494.

Laird, N. P., 1969, Anomalous temperature of bottom water in the Panama Basin: Jour. Mar. Res., v. 27, no. 3, p. 355-357.

Laird, N. P., 1971, Panama Basin deep water - properties and circulation: Jour. Mar. Res., v. 29, no. 3, p. 226-234.

Lamb, H. H., 1970, Volcanic dust in the atmosphere with a chronology and assessment of its meteorological significance: Phil. Tran. Roy. Soc. Lond., v. 266, p. 425-533.

Lisitsin, A. P., 1971, Distribution of carbonate microfossils in suspension and in bottom sediments: In Funnel, B. M. and W. R. Riedel (eds.), The Micropaleontology of Oceans, Cambridge University Press, Cambridge, p. 197-218.

Lisitsin, A. P., 1972, Sedimentation in the world's oceans: SEPM Special Publication No. 17, 218 p.

Lonsdale, P., W. R. Normark, and W. A. Newman, 1972, Sedimentation and erosion on Horizon Guyot: Geol. Soc. Am. Bull., v. 83, p. 289-316.

Luz, B. and N. J. Shackleton, 1975, $CaCO_3$ solution in the tropical East Pacific during the past 130,000 years: In Dissolution of Deep-Sea Carbonates, Special Publication No. 13, Cushman Foundation for Foraminiferal Research, p. 142-150.

Moore, T. C., Jr., 1970, Abyssal hills in the Central Equatorial Pacific: sedimentation and stratigraphy: Deep-Sea Res., v. 17, p. 573-593.

Moore, T. C., Jr., G. R. Heath, and R. O. Kowsmann, 1973, Biogenic sediments of the Panama Basin: Jour. Geol., v. 81, p. 458-472.

Morse, J. W. and R. A. Berner, 1972, Dissolution kinetics of calcium carbonate in sea water: II. A kinetic origin for the Lysocline: Amer. Jour. Sci., v. 272, p. 840-851.

Muller, R. H., 1966, Specialized analog computer resolves overlapping peaks: Analytical Chem., v. 38, p. 121A-123A.

Ninkovich, D. and N. J. Shackleton, 1975, Distribution, stratigraphic position and age of ash layer "L" in the Panama Basin region: Earth Planet. Sci. Lett., v. 27, no. 1, p. 20-34.

Nowroozi, A. A., M. Ewing, J. E. Nafe, and M. Fliegel, 1968, Deep ocean current and its correlation with the ocean tide off the coast of northern California: Jour. Geophys. Res., v. 11, p. 1921-1932.

Odén, S., 1915, Eine neue Methode zur mechanischen Bodenanalyse. Internat. Mitt. Bodenk., v. 5, p. 257-311.

Oser, R. K., 1972, Sedimentary components of Northwest Pacific pelagic sediments: Jour. Sed. Petrology, v. 42, no. 2, p. 461-467.

Pak, H. and J. R. V. Zaneveld, 1973, The Cromwell Current on the east side of the Galapagos Islands: Jour. Geophys. Res., v. 78, no. 33, p. 7845-7859.

Plank, W. S. and J. R. V. Zaneveld, 1973, The distribution of suspended matter in the Panama Basin: Jour. Geophys. Res., v. 78, p. 7113-7121.

Prospero, J. J. M. and E. Bonatti, 1969, Continental dust in the atmosphere of the Eastern Equatorial Pacific: Jour. Geophys. Res., v. 74, p. 3362-3371.

Rex, R. W. and E. D. Goldberg, 1958, Quartz content of pelagic sediments of the Pacific Ocean: Tellus, v. 10, p. 153-159.

Rhoads, D. C., 1970, Mass properties, stability and ecology of marine mud related to burrowing activity: In Grimes, T. P. and J. C. Harper (eds.), Trace Fossils, Geol. Jour. Special Issue No. 3, p. 391-406.

Rhoads, D. C. and D. K. Young, 1970, The influence of deposit feeding organisms on sediment stability and community structure: Jour. Mar. Res., v. 28, p. 150-178.

Richards, A. F., 1965, Geotechnical aspects of recent marine sediments, Oslofjord, Norway (abst.): Bull. Am. Assoc. Petrol. Geol., v. 49, p. 356.

Sandstrom, H., 1966, The importance of topography in generation and propagation of internal waves: Ph.D. Thesis, San Diego, University of California, 105 p.

Sandstrom, H., 1969, Effects of topography on propagation of waves in stratified fluids: Deep-Sea Res., v. 16, p. 405-410.

Seilacher, A., 1967, Bathymetry of trace fossils: Mar. Geol., v. 5, p. 413-428.

Stevenson, M., 1970, Circulation in the Panama Bight: Jour. Geophys. Res., v. 75, no. 3, p. 659-672.

Stevenson, M. R. and B. A. Taft, 1971, New evidence of the Equatorial Undercurrent east of the Galapagos Islands: Jour. Mar. Res., v. 29, no. 2, p. 103-115.

Terry, R. A., 1956, A geological reconnaissance of Panama: Calif. Acad. Sci., Occas. Pap. 26, 91 p.

Truchan, M. and T. Aitken, 1973, Site surveys (DSDP 155 and 158) on the Coiba and Cocos Ridges in the Panama Basin: In Initial Reports of the Deep Sea Drilling Project, Washington, D. C. (U. S. Government Printing Office), v. 16, p. 473-496.

U. S. Navy, 1959, Marine Climatic Atlas of the World, v. 5, South Pacific Ocean.

van Andel, Tj. H., 1973, Texture and dispersal of sediments in the Panama Basin: Jour. Geol., v. 81, p. 434-457.

van Andel, Tj. H., G. R. Heath, B. T. Malfait, D. F. Heinrichs, and J. I. Ewing, 1971, Tectonics of the Panama Basin, Eastern Equatorial Pacific: Geol. Soc. Am. Bull., v. 82, p. 1489-1508.

Wilde, P., 1966, Quantitative measurements of deep-sea channels on the Cocos Ridge, East Central Pacific: Deep-Sea Res., v. 13, p. 635-640.

Wunsch, C., 1969, Progressive internal waves on slopes: Jour. Fluid Mechanics, v. 35, p. 131-144.

Wyatt, B., W. Gilbert, L. Gordon, and D. Barstow, 1970, Hydro0 graphic data from Oregon waters, 1969: Data Report 42. School of Oceanography, Oregon State University, Ref. 70-12, 155 p.

Wyrtki, K., 1965, Surface currents of the Eastern Tropical Pacific Ocean: Bull. Inter-Amer. Tropical Tuna Comm., v. 9, no. 5, p. 271-304.

Yamashiro, C., 1975, Differentiating dissolution and transport effects in foraminiferal sediments from the Panama Basin: In Dissolution of Deep-Sea Carbonates, Special Publication No. 13, Cushman Foundation of Foraminiferal Research, p. 151-159.

APPENDIX

APPENDIX

Silt-Size Modal Analyses: Method

Surface sediment samples from 20 multiple gravity cores were placed in 8 oz. jars and tumbled slowly for five hours. As both wet and dry samples were used, test samples (wet, freeze-dried, heat dried and air dried) were run to see if the initial state of the sediment or the additional tumbling time needed by the dry samples was significant. No significant differences in the mode percentages were found. To aid in dispersion, a few drops of Calgon were added to the sample. The organic content of the sediment was negligible.

The dispersed sediment was decanted at 63 microns using standard settling techniques, assuming Stokesian settling. The greater than 63 micron fraction was then dried and weighed. The finer fraction was made up to volume (100 ml) and 5 cc was pipetted off, dried and then weighed to determine the total silt and clay-sized fractions.

The less than 2 micron fraction was decanted, freeze-dried and weighed. The 2-63 micron (9-4ϕ) material was then analyzed using the Cahn Electrobalance (Dauphin, 1972).

The analog data was digitized at 0.1 ϕ intervals corresponding to settling times calculated from Stokes Law as follows:

$$t = \frac{K}{D^2}$$

where D is the particle diameter and K is a systems constant:

$$K = \frac{0.3\, h\, \eta\, 10^8}{(d_p - d_f)\, g}$$

where h = column height in centimeters (25 cm)

η = viscosity of the sedimentation fluid in poises

d_p = assumed density of particles in g/cm^3 (quartz)

d_f = density of sedimentation fluid g/cm^3 (water)

g = acceleration due to gravity in cm/sec^2

Oser (1972) demonstrated that this continuous sedimentation technique has a reproducibility of 0.2 ϕ units.

The cumulative particle size distribution was calculated by a single numerical differentiation of a cubic spline curve fitted to the raw data (Odén, 1915) and the frequency distribution was determined by a second differentiation. The raw data was smoothed by including a five point averaging window and a smoothing cubic spline function f(x) such that:

$$\sum^{N} i = 1 \left(\frac{f(xi) - yi}{dy_i} \right)^2 \leqslant S$$

and

$$\left| \int_{x_1}^{x_n} \left[f''(\xi) \right]^2 d\xi \right| \quad \text{is a minimum}$$

where ξ is the data set.

The recommended range is $N - \sqrt{2N} \leq S \leq N \pm \sqrt{2N}$, where N is the number of data points (50) (M. Clauson, T. Chriss, S. Swift, and N. Pisias, personal communications). The value chosen for this study was 43. Zero and 3 point averages and $S = 0$ were also used as test runs but no significant differences were found in the mode percentages while the curves were not as easily resolved. A computer program written by M. Clauson, S. Swift, and N. Pisias for the Control Data Corporation 3300 computer performs the appropriate numerical differentiations; the output is in the form of plots of cumulative and frequency curves.

The polymodal distribution was resolved using a duPont 310 curve resolver (Muller, 1966; Dauphin, 1972) with six operating channels programmed to generate Gaussian functions. Eight modes were recognized so they were resolved in two stages, with the four overlapping modes giving consistancy to the technique.

The modes were grouped according to natural clusters that were observed from a histogram of the mode positions (Fig. 18) (Modes A1-2, B1-3, C1-3, Fig. 16). Most samples have one mode per cluster, with occasionally a small tail mode. The actual positions of the peaks vary by as much as 0.5 ϕ from one sample to the next, but each cluster appears to be approximately normally distributed. The test samples showed similar variability, but the relative

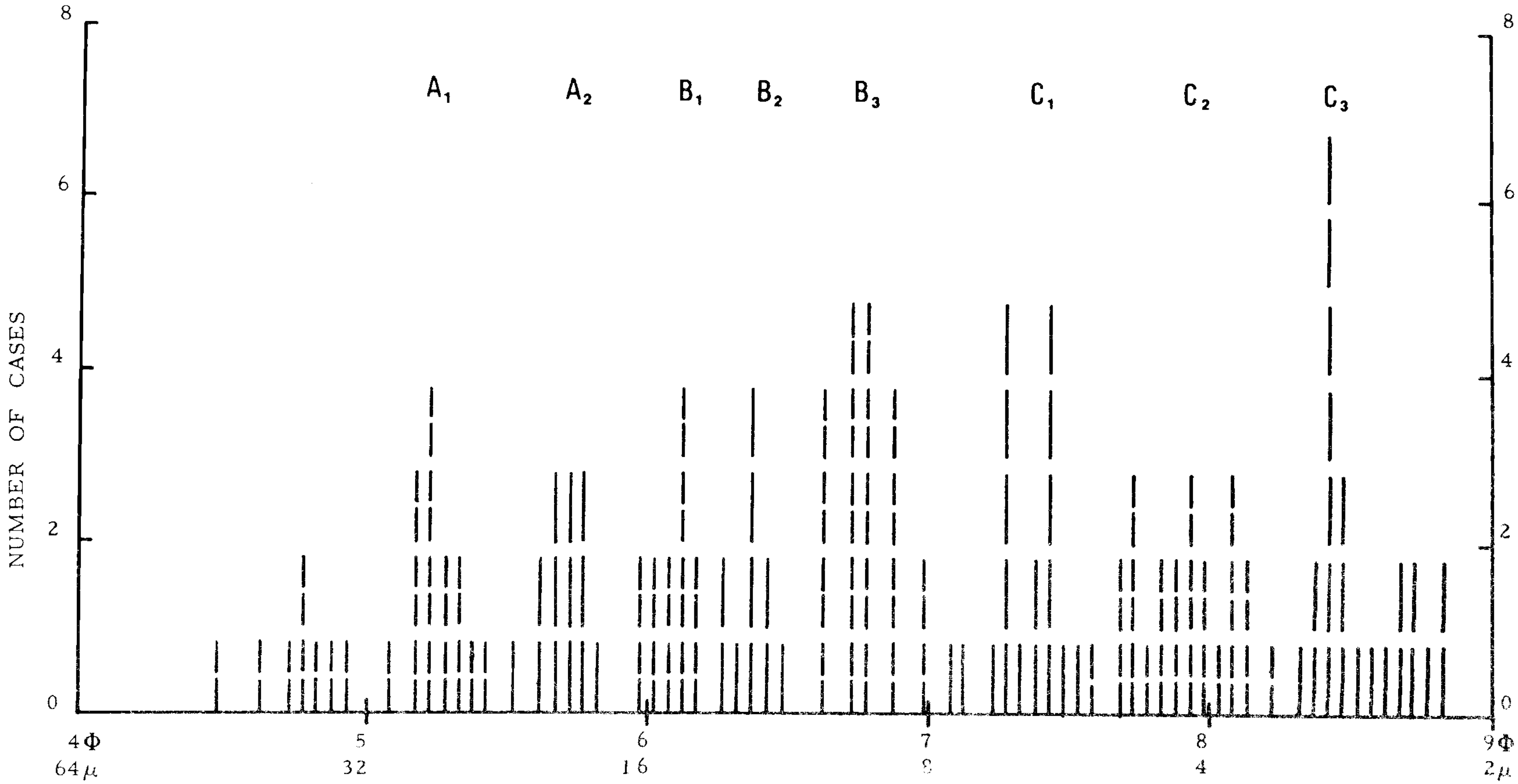

Figure 18. Histogram of number of cases in each 0.05Ø interval vs. grain size. Clusters have been shown alternatingly with broken and solid bars. Letters indicate modes mentioned in the text.

percentages of the modes within each group were consistant, with a variability of about ± 3% of the total material. The modes were expressed as weight percent of the total silt-sized fraction to avoid the masking effect of the coarse and fine fractions. The mode percentages were then mapped.

The procedure is summarized as follows:

1. tumble sediment for 5 hours.
2. decant at 63 micron → dry, weigh > 63 micron fraction.
3. make the < 63 micron fraction up to volume (100 ml).
4. pipette off 5 cc → dry, weigh.
5. decant at 2 micron → freeze dry, weigh < 2 micron fraction.
6. do Cahn analysis on 2-63 micron fraction.
7. compute frequency distribution from analog output.
8. curve resolve modes.
9. map relative percentages of individual modes.